18 June 1935

NRL Report No. H-1159.

NAVY DEPARTMENT

BUREAU OF ENGINEERING

Report on

FR-1159

A Photoelastic Investigation of the Stress Concentrations in Longitudinal Sections of Corrugated Pipe
for U.S. Naval Experiment Station, Annapolis, Md.

NAVAL RESEARCH LABORATORY
ANACOSTIA STATION
WASHINGTON, D. C.

Number of Pages: Text - 9 Plates - 37

Authorization: Director, Naval Research Laboratory.

Date of Test: July 1934 through May 1935.

Prepared by:

John A. Plugge, Contract Employee

Reviewed by:

E.O. Hulburt, Physicist, Supt. Div. of Physical Optics.

Approved by:

H.M. Cooley, Captain, U.S.N., Director.

Distribution:
Bu.Eng.(2)
Eng.Exp.Sta.(3)

ts

TABLE OF CONTENTS

Appendices

ABSTRACT

This photoelastic investigation has dealt with stresses in longitudinal sections of corrugated pipe. The work has been supplementary to a broader problem which has been conducted at the Engineering Experiment Station, Annapolis, Maryland. The work at that Station on corrugated pipe comprised physical tests on steel pipe and stress analysis by the analytical methods of the theory of elasticity.

The cooperative work has included tests on models of sections from two samples of pipe submitted by the Experiment Station. It has also included a study of the maximum stress in each of a series of seven theoretically designed models in which the curvature of the corrugation was the only variable, and another series of 3 models in which the depth of corrugation was the only variable.

The work shows that maximum stresses are not increased rapidly by moderate decreases in radius of curvature unless the radius is extremely small in proportion to the rest of the section. With a change of radius from 1.145 inches to 0.3125 ins. the maximum stress increased only from 1320 lbs. per sq.in. to 1620 lbs. per sq.in., while a change from 0.3125 inch to 0.0100 inch increased the maximum stress from 1620 lbs. per sq.in. to 2150 lbs. per sq.in. It also shows that an increased depth of corrugation has exactly the effect upon the maximum stress that would be predicted from ordinary analysis of the external forces and moments. This increase is uniform and in keeping with moment=force times distance.

AUTHORIZATION

1. This problem was authorized by the Director, Naval Research Laboratory. References (a) and (b) below preceeded the authorization of the problem.

Reference: (a) Director, Eng.Exp.Sta.ltr. NP16/L5/S48(G) of 19 June 1934.
(b) Director, N.R.L.ltr. N8-8/L5-2 of 3 July 1934.

STATEMENT OF PROBLEM

2. The Engineering Experiment Station has been engaged in an investigation of the strength and flexibility characteristics of corrugated steam piping. At that station physical tests on steel pipe and theoretical elastic analyses have been made.

3. The purpose of this investigation has been to determine by photoelastic methods the maximum edge stresses introduced by a longitudinal force, in possible shapes of corrugation which may be used in corrugated pipe. In obtaining this quantitative information, a relationship between maximum stress and geometrical variations of curves has been obtained. This may prove useful in determining optimum proportions of corrugation shapes in pipes.

4. The pipes tested included various shapes such as "straight tangents", quarter bends, and expansion bends, and were made of tubing having wall thicknesses of 0.280 and 0.288 inch and an outside diameter of 6.625 inches.

5. The preliminary tests conducted by the Engineering Experiment Station on this corrugated piping indicated that the actual stresses existing under load are considerably greater than would exist in an uncorrugated pipe of the same nominal diameter, the same dimensions, and under the same loading. The actual amount of stress multiplying effect had not been definitely determined.

6. It was believed that photoelastic methods would prove useful in solving some of the questions which arose through this investigation and that such a study would show more clearly just what was taking place in two dimensional corrugated sections.

7. The first phase consisted in the examination of models of sections of pipe submitted by two different manufacturers which had slightly different curves in the corrugations, and to measure quantitatively the relative stresses in these sections under the same loading.

8. The second phase consisted in the construction of two series of models, one to determine the relation between maximum stress and radius of curvature and the other to determine the relation between maximum stress and the depth of corrugation. In the first or "B" series, the pitch, depth of corrugation, and "thickness of metal" were kept constant. In the second or "C" series, the pitch, radius of the sharper curve, and "thickness of metal" were kept constant. However, in both series the "thickness of metal"

was constant throughout the length of each and every corrugated model. This, of course, was not true in the models of the actual corrugated pipe sections which are herein designated as the "A" series.

KNOWN FACTS BEARING ON THE PROBLEM

9. The Engineering Experiment Station, previous to the commencement of the photoelastic work, had tested a "straight tangent" section of nominal six-inch diameter corrugated pipe. The test comprised the vertical erection of corrugated pipe about 76 inches long havings its base securely anchored by means of a flange. A beam was fixed on the top of the "tangent", normal to the vertical axis, and a load applied vertically to the end of the beam. The distance from the pipe axis to the point of application of the load was 66 inches. With this testing arrangement, load deflection relations were obtained. The displacement of the pipe axis from the vertical, at the top of the pipe when under load, was taken as deflection. When, in each case, the equivalent length of smooth pipe to give the obtained deflection under a given load was calculated, the equivalent length for one tangent was 36% greater than for the other. A visual examination of the corrugations of each tangent shows that while the corrugations are at approximately the same pitch, they differ in slope.

10. The differing wall thickness was compensated for in the calculation by using the moment of inertia in each case applying to the actual wall thickness. Certain test results in alternating flexure of this piping indicated that the stress multiplying effect differs in the two forms of corrugations. The actual amount of this difference was not known.

11. It was believed, therefore, that photoelastic models of sections of these pipes would answer the questions left in doubt by the above tests. These models are herein designated as Series "A".

THEORETICAL CONSIDERATIONS

12. It has long been known, and has been confirmed by photoelastic analysis, that sharp notches in a member caused small areas to be very highly stressed by a comparatively small load. Acute or square corners and small fillets give much higher stresses than large filleted corners. Also, curved beams give higher stresses than straight beams. The general facts have been studied by methods of the theory of elasticity using various assumptions, and uncoordinated work by photoelastic methods may be found in numerous publications, but definite and accurate answers to the questions arising from this problem could not be considered as forthcoming from the books.

13. As the corrugated pipe being studied at the Engineering Experiment Station had a wall thickness of approximately 0.28 inch, and as the smallest pitch, which is equivalent to the greatest number of corrugations, convenient to manufacture is probably two and a half inches, several constants could be used in the theoretical series of models. It was decided to use at double scale, the following constants:

Pitch:	2-1/2 inches
Thickness of Metal:	0.280 inch
Slope of tangent, from direction of length, on side of corrugation:	60°

Also, in the "B" series, the depth of corrugation was fixed at 1-3/8 inches from the center lines of the metal thickness on the opposite curves, varying only the radius of curvature so far as the sharper curve was concerned. In the "C" series the above mentioned radius of curvature was fixed at 1/4 inch and the depth of corrugation was made the only variable so far as the sharper curve was concerned. In all models the load was placed on the geometrical center line of the model. This approximated the location of the load line for zero lateral deflection closely enough to prevent separate data from being distinguished if taken with the models restrained from lateral deflection under longitudinal load.

14. It is apparent that in the "C" series the maximum bending moment should vary directly and proportionately to the depth of corrugation or moment arm. To account for the "C" series curve of maximum stress and depth of corrugation not passing through the origin (see Plate 10) after correcting the maximum stress for the uniform stress caused by the load on the models, the following correction must be introduced. Using the following symbols:

f' = measured stress at extreme fiber
f = fiber stress due to pure bending
M = moment on section
C = direct stress
L = moment arm (actual)
P = load
k = constant

Now, as the stress is not due entirely to pure bending, assume

$f' = f + C$ and $f = kM$

$\therefore f' = kM + C$

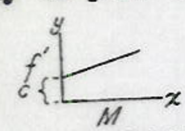

Now $M = PL$ (1/2 Amplitude = L + a shift of the "Neutral Axis", or P-Q = 0 line, due to the direct stress.)

As P is constant, we may plot the abscissa as L

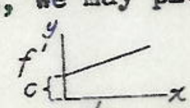

15. Photographs of the (P-Q=0) line show L to be a constant subtracted from one-half of the amplitude. The constant shift of this line under a load increment of 20 pounds = 0.079 inch.

L = 1/2 amplitude - 0.079"
i.e. $M = P \times (L - 0.079")$ or $M = 0$ when $L = 0.079"$ and a value of f' with only direct stress present or C = 143 lbs./sq.in.
$\therefore$ if L is plotted as abscissa and f' as ordinate $L = 0.079"$ at f' = 143 lbs./sq.in.
Hence Amplitude = 0.158" at f' = 143 lbs./sq.in.

This "C" series curve should, therefore, fit this point and at the same time be a straight line. It will be seen on Plate 10 that this is very nearly the case.

16. The central black line in a simple beam would be a true neutral axis, or to use better terminology, neutral line or edge view of the neutral plane. That black line in these curved beams is present because it is due to the principal stresses at all points along that line being equal or, in other words, P-Q=0, and the optics of the method give all such points as black or zero interference of the light. It does not follow that this is a true neutral line in the curved beams, for to have a true neutral line (P-Q) must not only equal zero, but each of the principal stresses must be in a direction at forty-five degrees to this neutral line. This condition gives maximum shear and zero longitudinal strain, but here with the principal stresses lying along and normal to the black line, the shear is zero and the longitudinal strain whatever is caused by principal stress P. This will be clear from Plate 22.

17. In pure bending, a straight beam can have a true neutral line only because both P and Q are each equal to zero along a central line, for in the case of pure bending their directions are also along and normal to this line, and hence the shear is zero in all directions about any point in the neutral line.

18. Plate 22 shows the results of the work that was done to illustrate the internal stress distribution across the section of symmetry on the sharper curve of A2. The only known data were the location of the point where P-Q=0 and the value of the edge stresses at points "a" and "u". Several assumptions were tried and finally a linear change of the radius from each edge to the point "k" where P-Q=0 combined with the assumed curve of P-Q shown on Plate 22 gave a quite reasonable solution. The radius at "k" was proportioned between the maximum and minimum values of the radius*, i.e. between r_a and r_u. The scale used was ten to one over the celluloid which would be twenty to one over the steel. (Note the measure indicated on the plate to be reduced equally with the drawing). The small error in continuity of the P and Q curves, as they approach their inevitable intersection, at P-Q=0, since the assumed P-Q curve was drawn through this known point, is evidence toward their being the correct curves of P and Q values. However, it is believed that that is incorrect, but as at first glance it appears (with the above mentioned small error showing) to be nearly perfect, it may mislead. The small error proves that the assumed P-Q curve across the section is very close to a possible P-Q curve to fit the known edge values of P-Q and the photoelastic location of P-Q=0; and then give continuous P and Q curves when integrated toward "k" from each edge. It seems that there are innumerable curves which would do these things and yet not be correct. The reason is that this P-Q curve can not be correct unless the difference of the areas under the compression and tension sides of the P curve is equal to the load on the specimen. That is merely $\Sigma F_y = 0$. ΣM about the intersection of the twenty pound load line and the Q stress line (i.e. the section "au") must also equal zero, but what that gives is immaterial until the other condition of static equilibrium $\Sigma F_y = 0$ is fulfilled. Plate 22 not only does not show a condition of static equilibrium, but also does not show pure bending, hence so close a check between the point where P = 0 and the point just above, found from the solution according to the curved beam theory as presented by Timoshenko in his "Theory of Elasticity", could not have a full meaning. The twenty pound direct load used is equal to 113 lbs. per sq. inch tension in the direction of P. Therefore, the line of P=0, i.e. "aku", should be shifted 1.13 inches to the left for the pure bending base line of the P curve. A shift in this direction will shift the point of P=0 still farther from the theoretical P=0 point unless the P curve is changing infinitely fast over the 1.13 inches, which is not beyond the realm of the possible. However, it seemed foolish to attempt any further manipulation in a solution which as yet is not in static equilibrium.

19. The equation used $\frac{\partial P}{\partial S_1} = - \frac{P-Q}{\rho_2}$ to integrate across the section will be found in Coker and Filon, "Photoelasticity", page 144.

PREPARATION AND PHOTOGRAPHS OF MATERIALS

20. When the possibilities of a photoelastic study of the various sections with which this problem was concerned were under consideration, a few preliminary models were made. These models were cut and filed entirely by hand to the same size as the pipe segments. An examination of these showed the expected high stresses on the concave side of the sharper curves and also that a larger scale model would be highly desirable for accurate quantitative measurements. These preliminary tests also indicated that it would be well worth while to examine the maximum edge stresses by this method.

21. The material used in all of the models was celluloid of one-quarter inch nominal thickness.

22. The design of the models of the steel corrugations submitted by the Engineering Experiment Station comprised merely the taking of accurate measurements along the steel shape. These are the "A" series. For model A-1 one hump was measured and this was used in series three times. For A-2 the three humps are each like the respective ones in the sample submitted. These models were made by hand and as the accuracy and smoothness of these curves was of primary importance, extreme care was exercised, but attempts to determine stresses at the very edge showed the need for edges which were more sharp (square) with surfaces more nearly flat. The continuity of the curves also was open to some little improvement. The need for such fine edges in this problem was due not only to the chief interest lying in the extreme fibers, but also because the difference to be measured (see plots of B and C series, Plates 3 and 10) between specimens was of a low order. However, the mechanical method of cutting the models which is described in Appendix A was devised and worked most satisfactorily. The accuracy obtained in the models was approximately plus or minus one one-thousandth of an inch from the desired dimensions.

DESCRIPTION OF EXPERIMENTS

23. The models or specimens were, in turn, placed in the ten-inch beam of polarized light of the photoelastic apparatus. They were suspended from cross pivots at the top of a steel frame and dead weights accurate to 0.1 gram in ten pounds were used to load them.

24. All measurements were taken in circularly polarized light while the A-2 isoclinic lines were, of course, taken in plane polarized light.

25. The isoclinics (Plate 21) were drawn on a screen upon which the image of the specimen was projected. The crossed Nicol prisms were rotated in the direction shown by the arrow on the above plate, in increments of ten degrees. The photographs of Plates 23 to 25 show the individual A-2 isoclinic lines, the composite of which appears on Plate 21. These lines are lines of equal direction of principal stress. The optics of the photoelastic

method have been explained in numerous publications and hence will not be repeated here. From these isoclinic lines to the lines of principal stress, also shown on Plate 21, is merely a drafting operation. The principal stress lines may be as sparse or well filled in as desired. It was unnecessary to extend the lines beyond the points shown on the drawing completely to illustrate the directions of the principal stresses in that locality. Had a study of the internal stresses been a part of this problem, it would have been well to have spaced the lines of principal stress so as to make the included strip between any two adjacent lines carry equal loads. This would have shown a concentration of lines of principal stress where there is a high stress intensity. However, in this work there are no internal quantitative data, hence the lines shown indicate directions only and do not tell anything quantitatively nor does any grouping of lines indicate a concentration of stress. The grouping of the lines for a short distance along the sharper curve on the isoclinic drawing shows the locus of points where P-Q=0, i.e. where the principal stresses are equal. More has been said about this under the section "Theoretical Considerations".

26. The data tabulated in Plate 14 for the "A" series and in Plate 15 for the "B" and "C" series and plotted in Plates 1 to 13 were taken with a tension strip, see Plate 36, used as an optical compensator. This tension strip, which was cut from the same sheet of celluloid as the models, was mounted in a tension frame and placed in the circularly polarized beam at a point where the beam was parallel. An image of the model was formed at this same point and hence when the tension strip was focussed on a screen, the images of both model and tension strip were superimposed, optically making two bodies occupy the same space at the same time. The tension strip was used to measure either tension or compression stresses because of the ease of keeping uniform tension throughout the area of the strip, whereas uniform compression would have been extremely difficult to maintain. As the ellipse of stress at a free edge on the model reaches the limiting case of a line, the greater axis or greater principal stress lying along the edge and the lesser axis or lesser principal stress being equal to zero, the edge stresses or extreme fiber stresses are either tension or compression parallel to the edge. The compensating strip must always lie along and normal to the principal stresses at a point. By compensating for the interference of the light in this manner, P-Q, the difference of the principal stresses was measured. Now, as one of the stresses is zero at a free edge, the compensation here actually measured the only stress present. To compensate for a tensile stress, the tension strip was placed perpendicular to the edge, while to compensate for a compressive stress, it was placed parallel to the edge.

27. The photographs of the models all showed a bright band along the edges. This was initial stress and is always a tension. To eliminate this from the results, differential readings were taken with the loaded and unloaded model. This method seemed better than trusting even a slightly imperfect annealing to eliminate this initial stress. In these models the initial edge stresses were quite high, but all low enough that satisfactory differentials could be taken above them. On models A-1 and A-2 where compression stresses were measured, it will be noted on Plates 1 and 2 that the compression stress did in no case completely overcome the initial tension. This, however, did not affect the accuracy of the measurements, though stresses of low order are as a rule more difficult to measure than high ones. Had there been no initial stress, the lower ends of the plots would be at the origin instead of in a positive direction on the abscissa. Positive slopes show tension and negative slopes compression stresses due to the applied load.

28. The shift of the (P-Q=0) black line from the centerline of the "metal thickness" at the peak of the sharper curve of models A-1; A-2 and C-1, B-4 is shown on Plate 20A. The dimensions were taken directly from photographic negatives. The right column shows the location of the (P-Q=0) line without the image of the tension compensating strip being superimposed upon the image of the stressed model. As this location was shifted when the tension strip was introduced, pictures were taken of this condition and are shown in the center column. The left column shows conditions when the tension strip was loaded sufficiently to just compensate for the direct stress due to the load on the model. Hence the change from the center to the left columns show the shift of the (P-Q=0) line due to direct stress, and when this correction is imposed upon the right column, the true position of the (P-Q=0) line for pure bending is obtained.

DISCUSSION OF RESULTS

29. The results of this experimental problem are contained in the plots of data, Plates 1 through 13, the data for which are tabulated in Plates 14 and 15.

30. Plates 1 and 2 (series A) show that the inside of either curve is stressed higher than the outside of either curve and that the highest stress intensity is located at the inside of the sharper curve. This is apparent from the greater slope of the stress-load curve for this point. A-1 shows an appreciably higher stress than is found for A-2 under similar loads.

31. Plates 4 to 9 inclusive and 11 through 13 each show the stress-load curve for a model of the B and C series. The lines drawn through the plotted points were arrived at in the following manner. A line, which appeared to be the best line through the points, was drawn and the stress intensity for a load increment of twenty pounds was plotted in a manner similar to Plates 3 and 10 for the B and C series respectively. Then the best curve for the B series was drawn in between points. From the very nature of this type of curve there are bound to be no discontinuities. From this curve the ordinates were read corresponding to the separate models, on the abscissa, and from this stress value the slope of the lines on the stress-load curves was determined. These lines are shown on the several plates and may be shifted parallel to themselves along the abscissa without changing their meaning. This method leaves all probable error in the individual plots to show up as the difference in slope of the line shown and that of the best straight line through the points. In nearly every case this is very small, in fact, almost a matter of opinion. This method prevents any wild points from influencing too heavily the slope of the line finally chosen. The straight lines show that the highest stresses obtained were still within the elastic limit of the material.

32. The B series curve of maximum stress vs. radius of curvature, Plate 3, shows that there is a small gradual and only slightly accelerated increase of stress intensity as the radius of curvature decreases from 1.145" for B-7 to about 0.312" for B-3. For smaller radii of curvature, the acceleration of increase of stress intensity is much greater, as shown by the sharp curvature of the curve from B-3 to B-1. Had sharper curves than that of model B-1 been studied, very much higher stress intensities would have been obtained. In fact, it appears that the B series curve would soon flow into

a region where the extreme concentrations and high intensities of notches would appear. The slight slope of this curve at the B-7 end indicates that the greatest radius tested is as large as there could possibly be any occasion to use in pipe to keep down the stress intensity, if it is worth while to use corrugations at all. However, point B-7, Plate 3, shows a stress intensity many times higher than would be found in an uncorrugated piece, tension strip, of the same dimensions under the same load.

33. **The C series curve, Plate** 10, was arrived at in a similar manner. **The point nearest** the origin is a theoretical point, the determination of which has been explained in section "Theoretical Considerations". The straight line through C-1, C-2 and C-3 passes through this point when extended. The straight line for this series was of course expected, since the lever arm of the applied force is the only variable. Also, the slope of this line is just that to be expected from the simple relation of moment equals force times lever arm as within the elastic limit the stresses are proportional to the moment.

CONCLUSIONS AND RECOMMENDATIONS

(a) Facts Established

(1) Bearing on the Problem.

34. The chief facts established by this problem are to be found in the two A series curves, Plates 1 and 2, and in the B and C series curves, Plates 3 and 10. These latter two show general facts, the generalization coming from data on specific cases. The results of tests on models A-1 and A-2, Plates 1, 2 and 14 show a lower stress than would be expected from those radii of curvature and depths of corrugation on the B and C series curves. This is due, however, to the thickening of the metal at the peak of the corrugation when the plain pipe is heated there and squeezed. This difference may prove an ample factor of safety over the theoretical or may be considered in corrugation design.

35. The B series curve shows that with the constants used throughout this series, the stress at the highest stressed point is not affected appreciably by a change of radius of curvature when the radius of curvature is large. Also, it shows that for smaller radii this change of stress is greater as the radius is decreased as well as the magnitude being higher. This increase in stress is marked for the conditions of this problem when the radius becomes less than 0.3 inch for the celluloid or 0.15 inch for the steel. Below 0.1 inch for the celluloid or one half of that value for the steel the stress increases so fast that smaller radii would be out of the question for corrugated pipe of the dimensions here considered.

36. From the C series curve one deduces the fact that the stress increases at a constant rate as the depth of corrugation is increased, and that this increase of stress is directly proportional to and equal to the increase of amplitude or depth of corrugation. As the maximum stress is proportional to the moment on the section and the moment equals the applied force times the lever arm, this is just as would be expected.

37. A study of the relative flexibility and extensibility of the models made for the photoelastic problem would doubtless give a valuable addition to the present work. It is therefore recommended that such a

study be made. Studies on the relations of side slope of corrugation, and thickness of metal at the crest with maximum stress, flexibility and extensibility would also doubtless furnish valuable information to be used in choosing corrugation shapes.

APPENDIX A

New Method of Cutting Transparent Models

A great many photoelastic models can be laid out directly on the celluloid, bakelite or other transparent material from which it is to be cut and often the cutting may be done entirely in lathes and milling machines. This is true where the edges are arcs of circles and straight lines with simple lines of construction. Where there are continuously changing curves and odd shapes added to the above, the model may often be finished by hand. This is perfectly satisfactory where great accuracy at every point is not necessary and where the chief interest lies within the interior of the model. A pair of three or five ply veneer wooden jigs, one clamped on either side of the model, have been used to good advantage where reasonably good edges have been desired from hand filing and scraping. This method and the common Dutch filing are good safeguards against serious gouges in the edge and edges far from flat and normal to the surfaces of the model. However, in the corrugated pipe models which were not only not simple geometric shapes but also designs in which the chief interest lay in the very edge fibers, the old methods of cutting failed to give satisfactory models even with the best workmanship. The following method using only one machine very satisfactorily solved this need for accurate models with smooth edges truly normal to the model surface and all curves joined in perfect continuity.

It was found that an eighth-inch diameter side milling tool used in the engraving machine (see Plate 37),if used at the normally high speed of the machine, would cut the edge desired. A generous supply of lard oil for lubrication aided materially in keeping the tool free from fused shavings. Also, the rate of cutting and the depth of cut should be kept at a minimum for best results. This method gave edges as free from initial stress as any previous method if due care was exercised.

At first it was hoped that the stylus could be guided along a large line drawing with sufficient steadiness to guide the cutting tool to produce a smooth edge on the model. In this trial a reduction of several times was obtained from the drawing to the model, nevertheless the increase of accuracy was not sufficient to overcome the unsteadiness caused by the pull of the cutting tool. After this attempt failed, a double scale drawing was made on sheet cooper using a sharp point. This scratch was then made a few hundredths of an inch deep, but like the first drawing, this guide was rendered inadequate by the pull of the tool. However, this last method was sufficiently good to indicate that the use of a harder material for the master and a loaded ball bearing in the groove might lead to a better technique.

A drawing of the shape was made four times the size of the corrugated pipe section which was to be studied. This drawing was dimensioned in such a manner (see Plates 16-20) that at the shop it could be duplicated on a sheet of one-eighth inch brass. A fine scratch line was used for the latter layout. This brass master was then cut out in the rough on a band saw and filed down to the scribed line and to dimension by hand. Great care was exercised in the final filing and micrometer measurements of dimensions were made almost continously along the curve. The brass, of course, being much more rigid and much more easily worked than any of the transparent materials used in photoelasticity, offered an opportunity for greater accuracy with an appreciable saving in time. Other important advantages were that,this being a master only, it did not require clamping in a manner to protect the surface from scratches, and also the edge did not have to be exactly square with the surface. This latter part is true, since the guide used along the edge followed only the highest points. The dimension between any two such points opposite one another being the one most easily read with a micrometer aided in promoting the accuracy.

In the event that a transparent model having more than one length of a given corrugation shape in tandem was to be made, this single corrugation alone had to be cut from brass. The ends of the master were cut normal to the length as a rule and always parallel to each other (see Plates 16 through 20). Hence, by sliding the master along its center line a distance just equal to its length after one corrugation had been cut, another just like it could be made as a continuation of the first. This was done for all but one model in this problem, namely A-2. Model A-2 required a full length brass master as shown in Plate 36.

The accuracy obtained in the masters was approximately plus or minus one thousandth of an inch. The finished model being made one-half the size of the master, or twice the size of the actual steel shape represented should have an error just one-half that of the master. This was approximately true, though the full advantage of reduction can not be obtained when a comparatively flexible material such as celluloid is being cut.

The master was mounted on a sheet of metal. The pin which followed around the edge of the master had twice the diameter of the side milling tool used to cut the model, which in this case made it one-fourth of an inch.

Though celluloid was used for the models shown on Plate 36, bakelite was tried for its adaptability to this method of cutting, and without any change of procedure gave the same excellent results obtainable in celluloid.

Pictures of the masters and models used for series "A", "B" and "C" will be found on Plate 36.

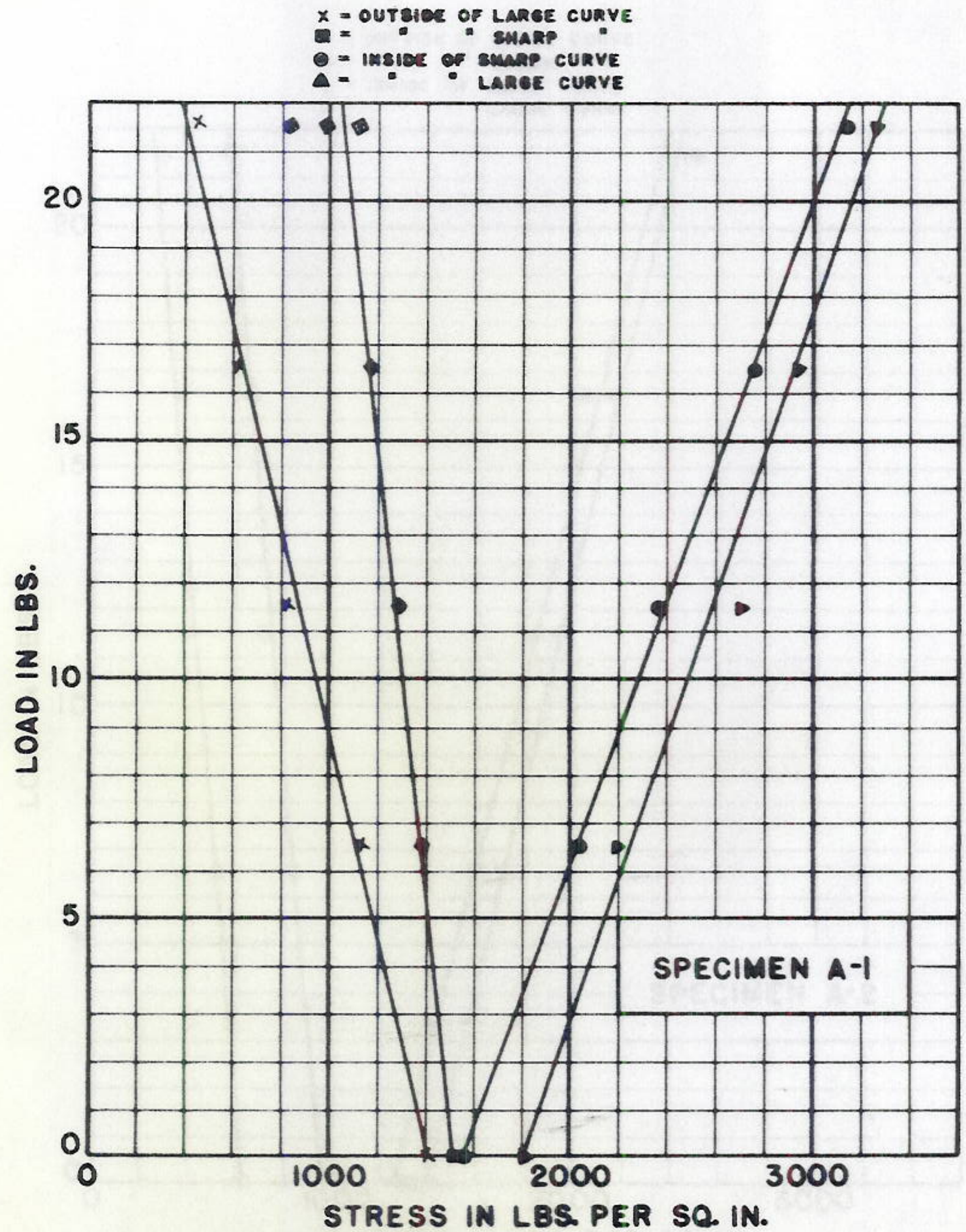

X = OUTSIDE OF LARGE CURVE
■ = " " SHARP "
● = INSIDE OF SHARP CURVE
▲ = " " LARGE CURVE
LOAD IN LBS.
0
5
10
15
20
0
1000
2000
3000
STRESS IN LBS. PER SQ. IN.
SPECIMEN A-1

PLATE 1

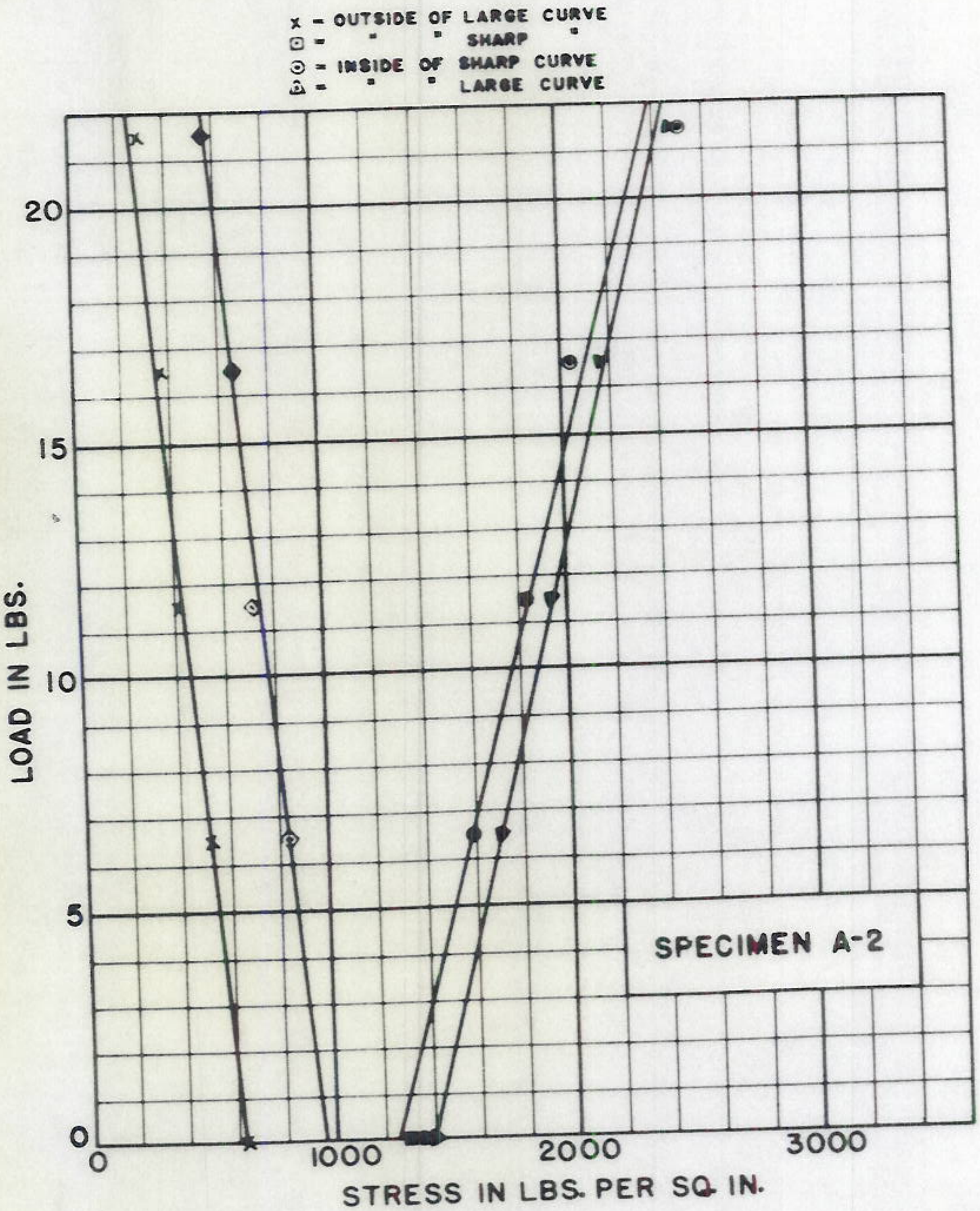
x = OUTSIDE OF LARGE CURVE
⊡ = " " SHARP "
⊙ = INSIDE OF SHARP CURVE
◬ = " " LARGE CURVE
LOAD IN LBS.
20
15
10
5
0
0
1000
2000
3000
STRESS IN LBS. PER SQ. IN.
SPECIMEN A-2

PLATE 2

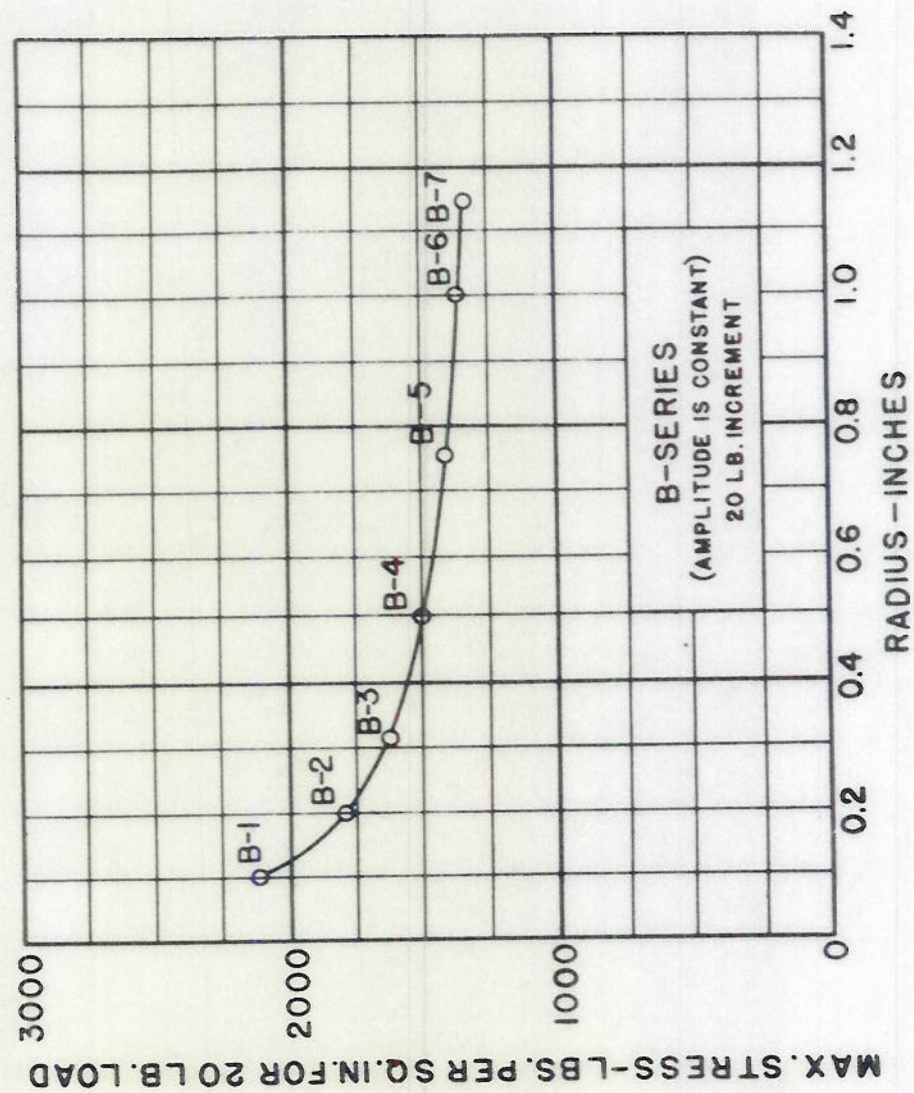
B-SERIES
(AMPLITUDE IS CONSTANT)
20 LB. INCREMENT
B-1
B-2
B-3
B-4
B-5
B-6
B-7
RADIUS-INCHES
0
0.2
0.4
0.6
0.8
1.0
1.2
1.4
MAX. STRESS-LBS. PER SQ. IN. FOR 20 LB. LOAD
1000
2000
3000

PLATE 3

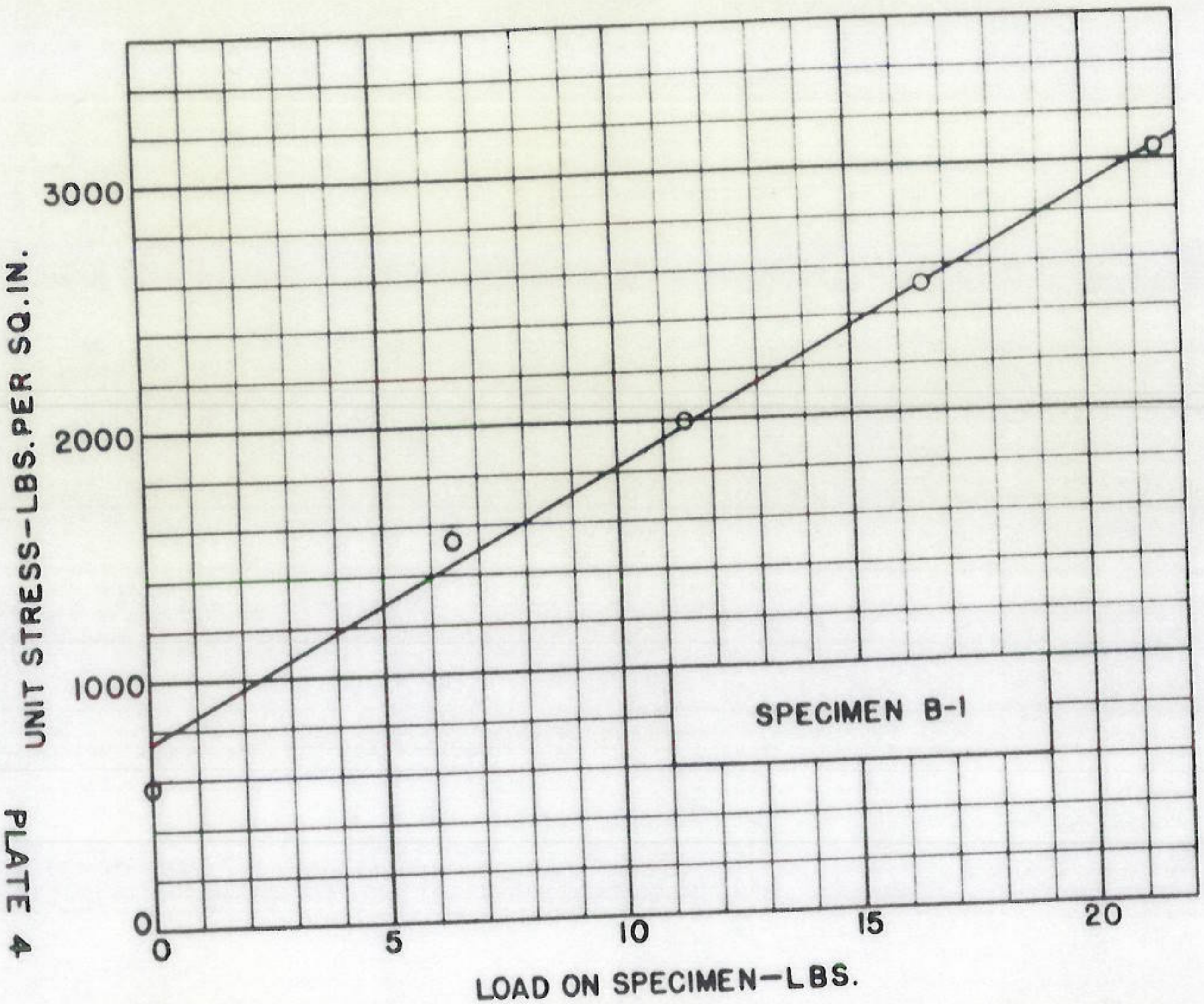
3000
2000
1000
0
UNIT STRESS-LBS. PER SQ. IN.
SPECIMEN B-1
0
5
10
15
20
LOAD ON SPECIMEN-LBS.

PLATE 4

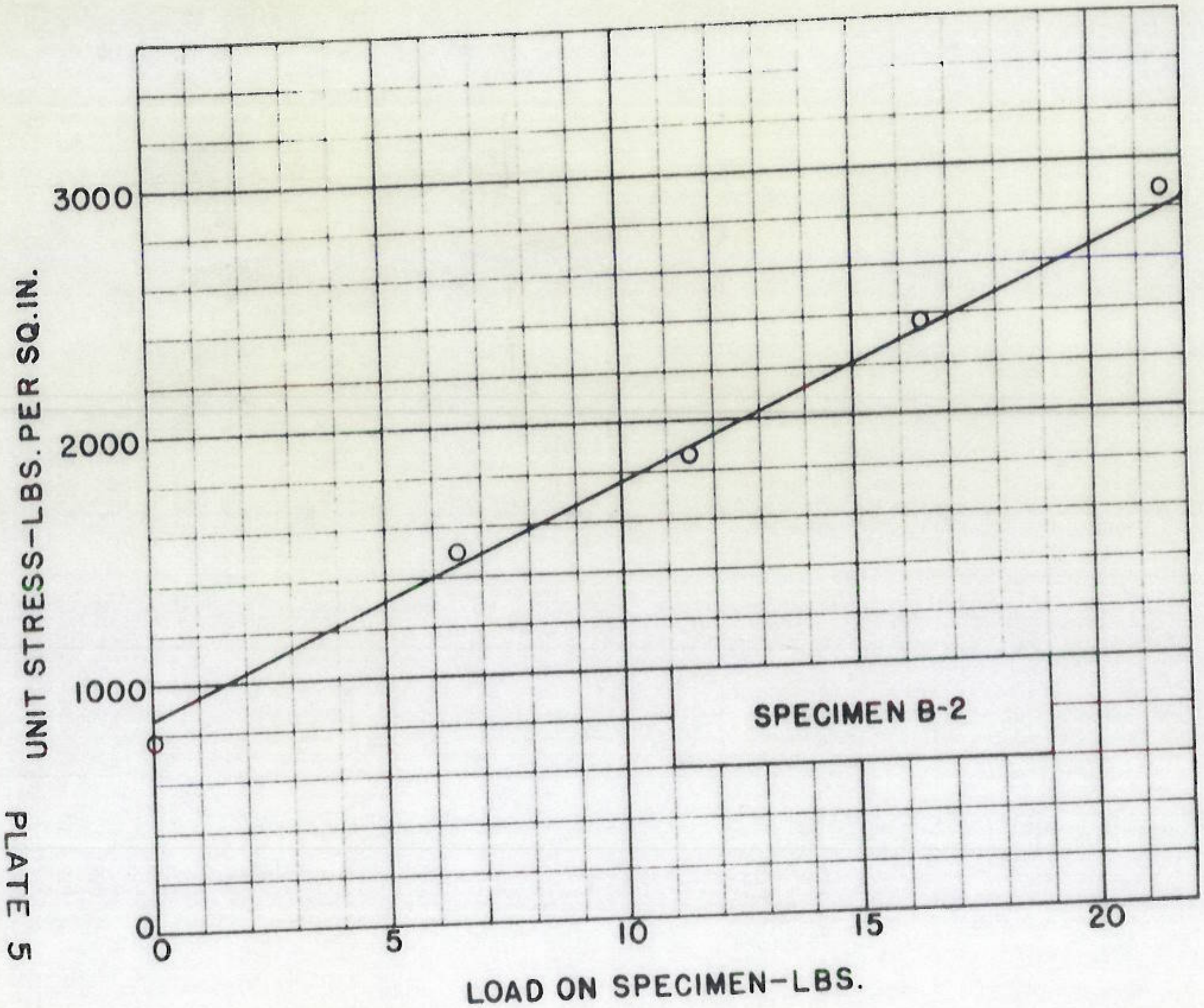
SPECIMEN B-2
UNIT STRESS-LBS. PER SQ.IN.
LOAD ON SPECIMEN-LBS.
3000
2000
1000
0
0
5
10
15
20

PLATE 5

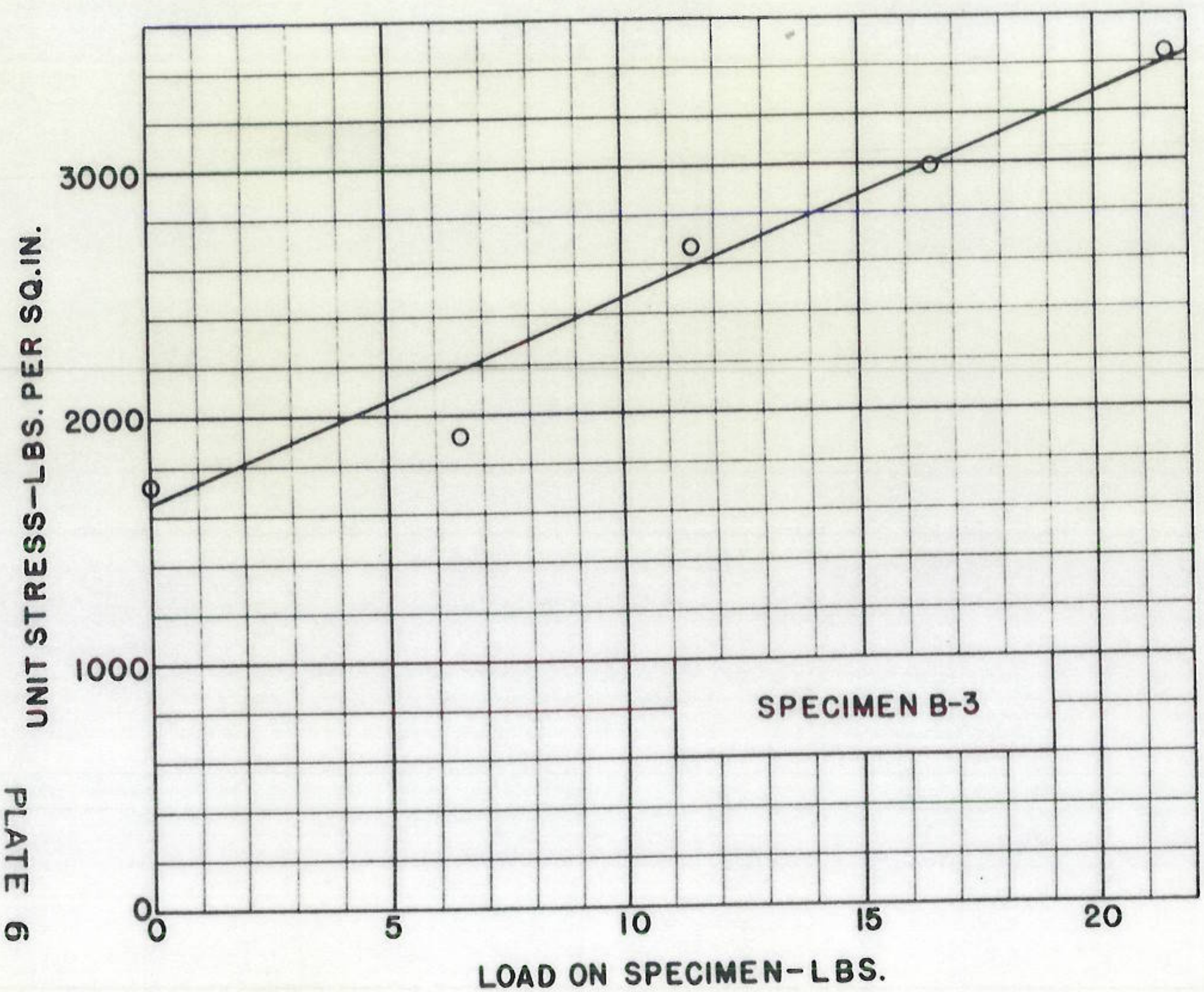

SPECIMEN B-3
UNIT STRESS–LBS. PER SQ.IN.
LOAD ON SPECIMEN–LBS.
3000
2000
1000
0
0
5
10
15
20

PLATE 6

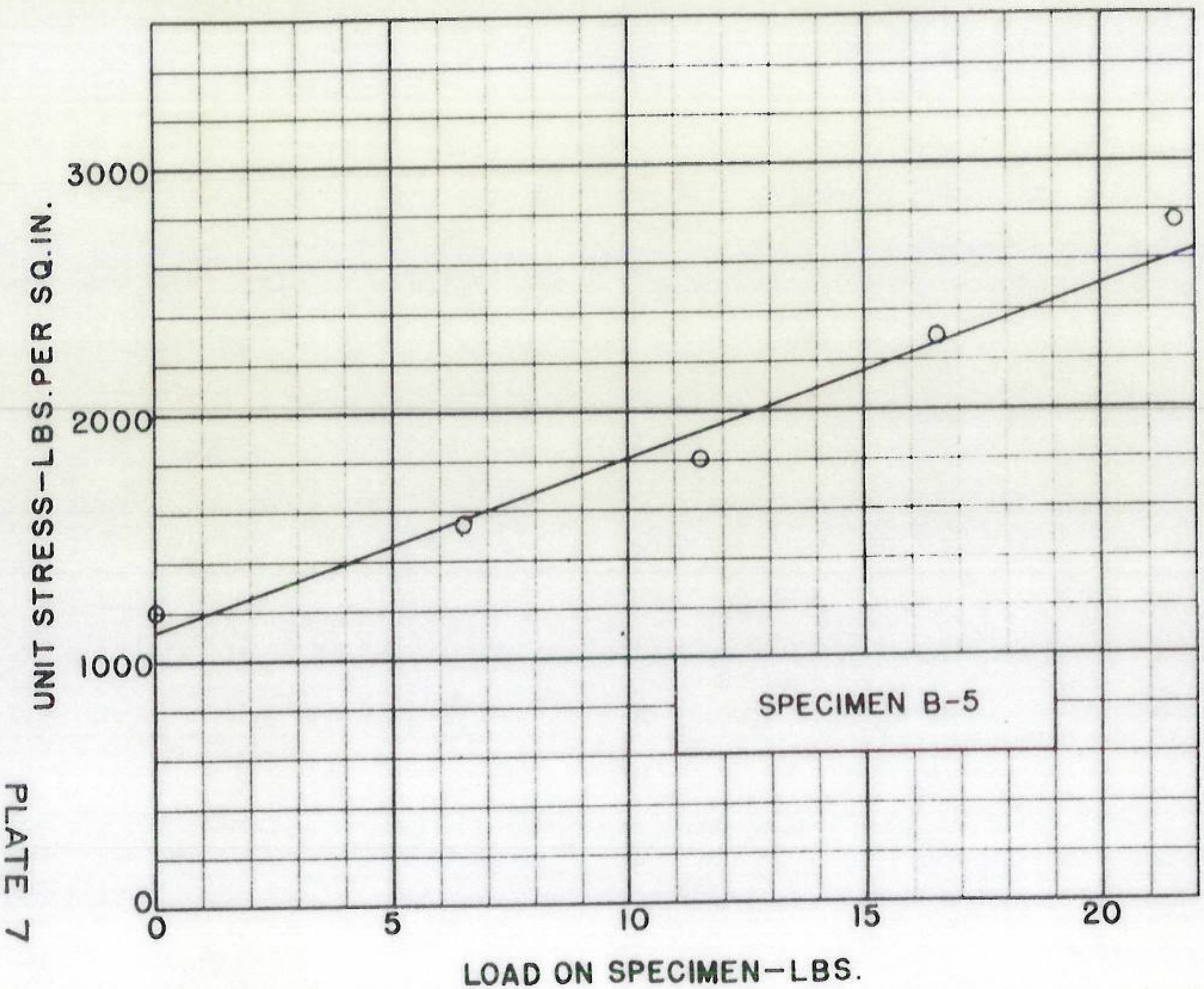
SPECIMEN B-5
UNIT STRESS-LBS.PER SQ.IN.
3000
2000
1000
0
0
5
10
15
20
LOAD ON SPECIMEN-LBS.

PLATE 7

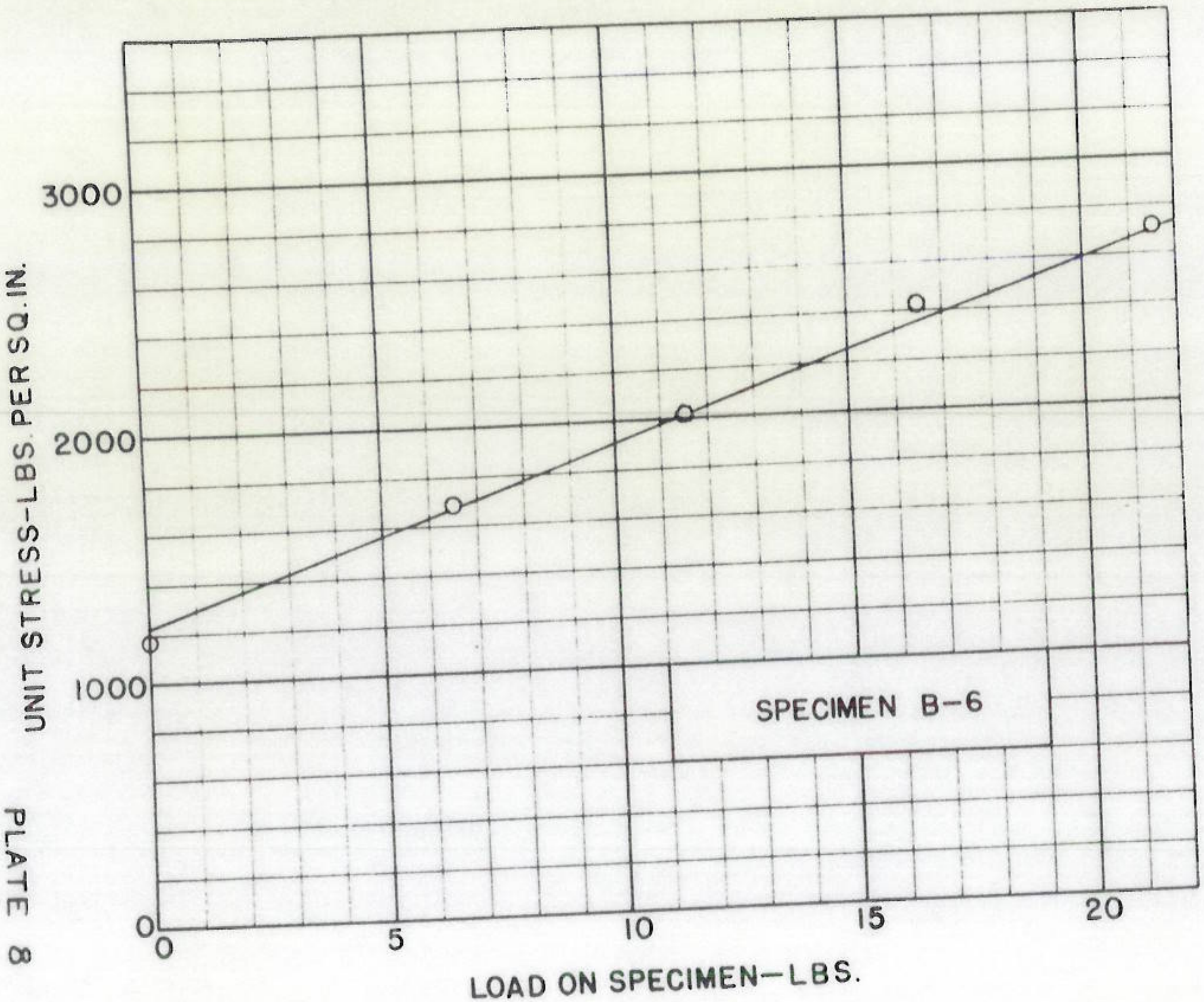

3000
2000
1000
0
UNIT STRESS-LBS. PER SQ. IN.
0
5
10
15
20
LOAD ON SPECIMEN—LBS.
SPECIMEN B-6

PLATE 8

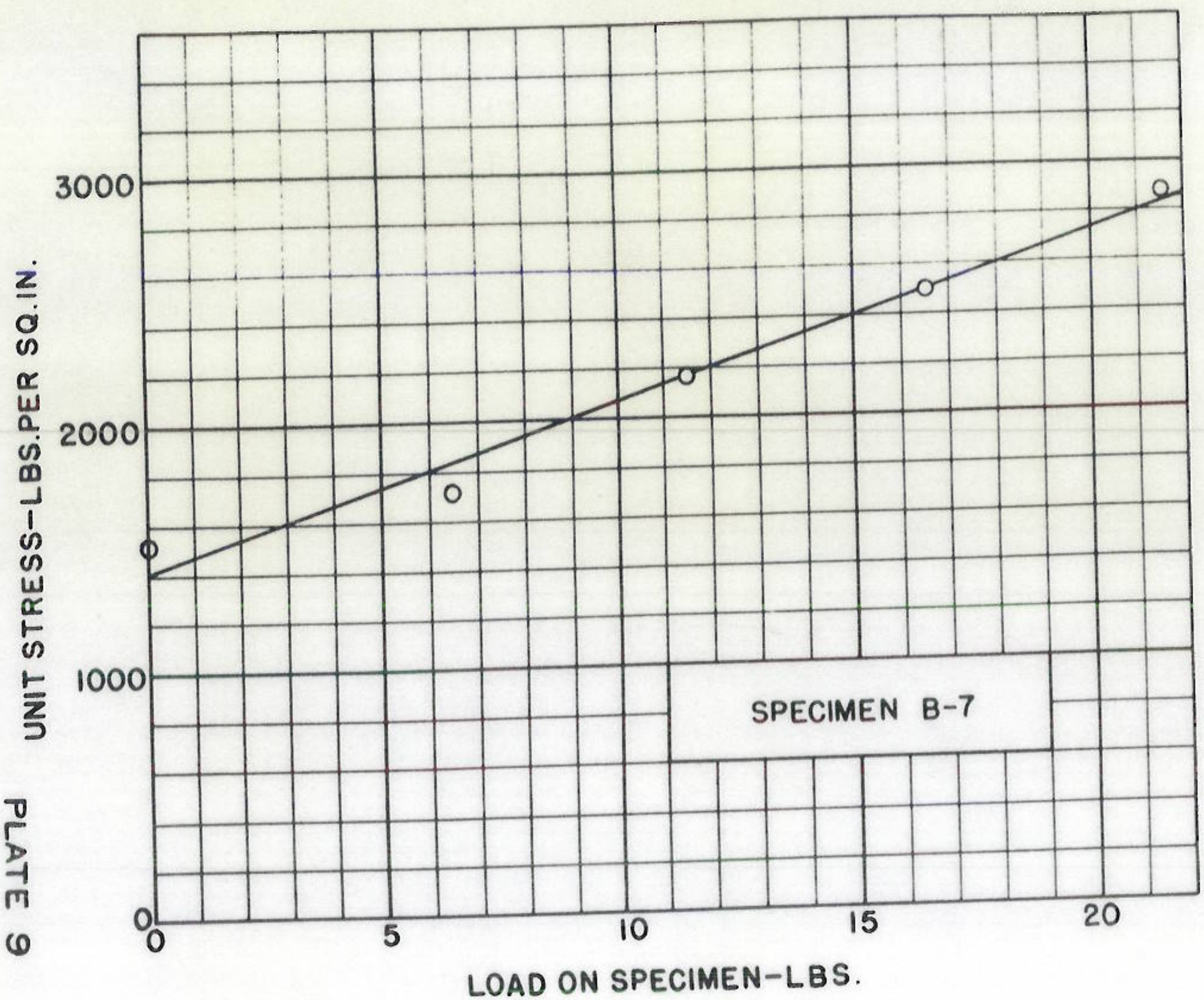
UNIT STRESS-LBS.PER SQ.IN.
3000
2000
1000
0
0
5
10
15
20
LOAD ON SPECIMEN-LBS.
SPECIMEN B-7

PLATE 9

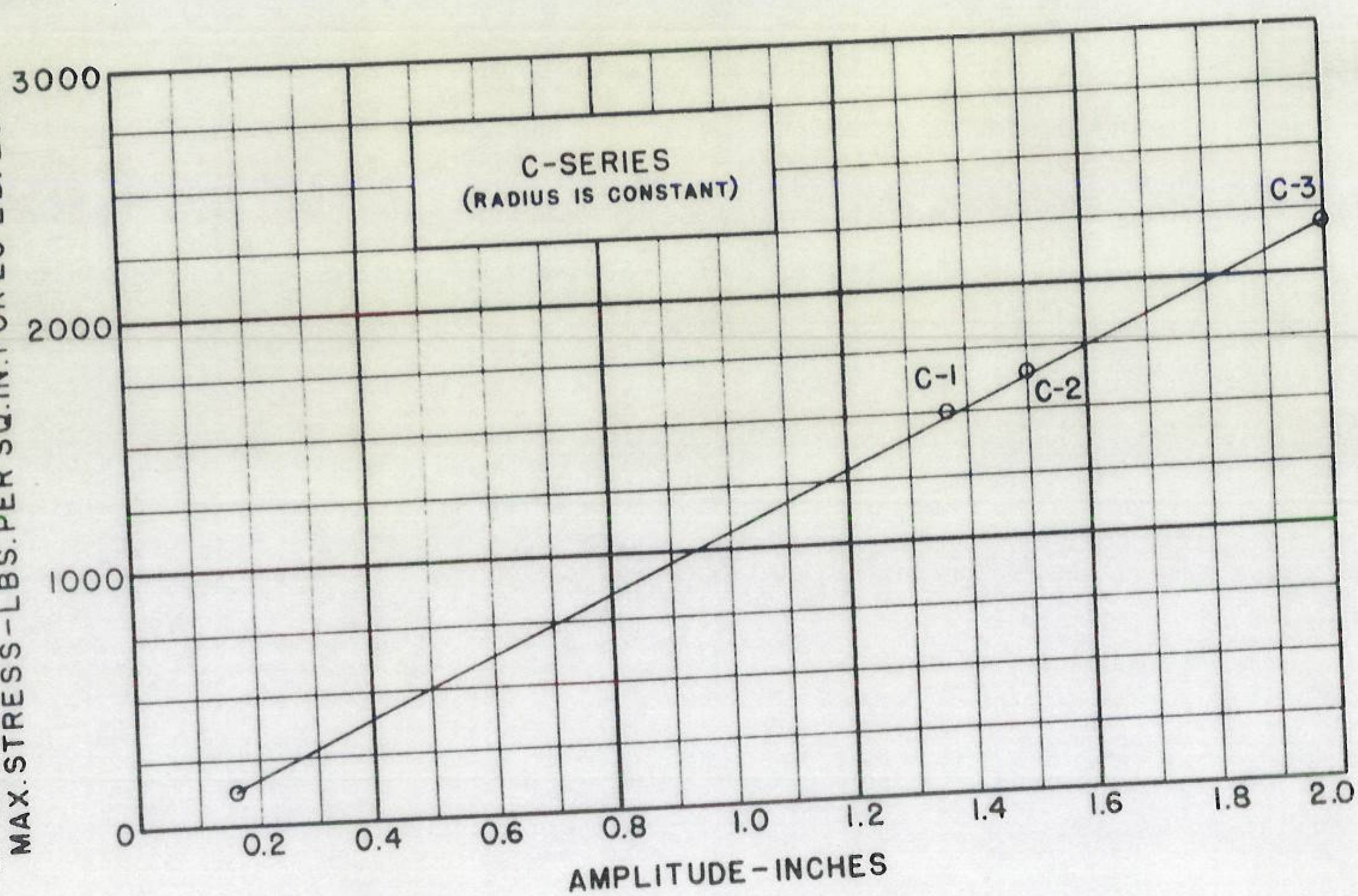
C-SERIES
(RADIUS IS CONSTANT)
C-1
C-2
C-3
MAX. STRESS-LBS. PER SQ. IN. FOR 20 LB. LOAD
0
1000
2000
3000
0.2
0.4
0.6
0.8
1.0
1.2
1.4
1.6
1.8
2.0
AMPLITUDE-INCHES

PLATE 10

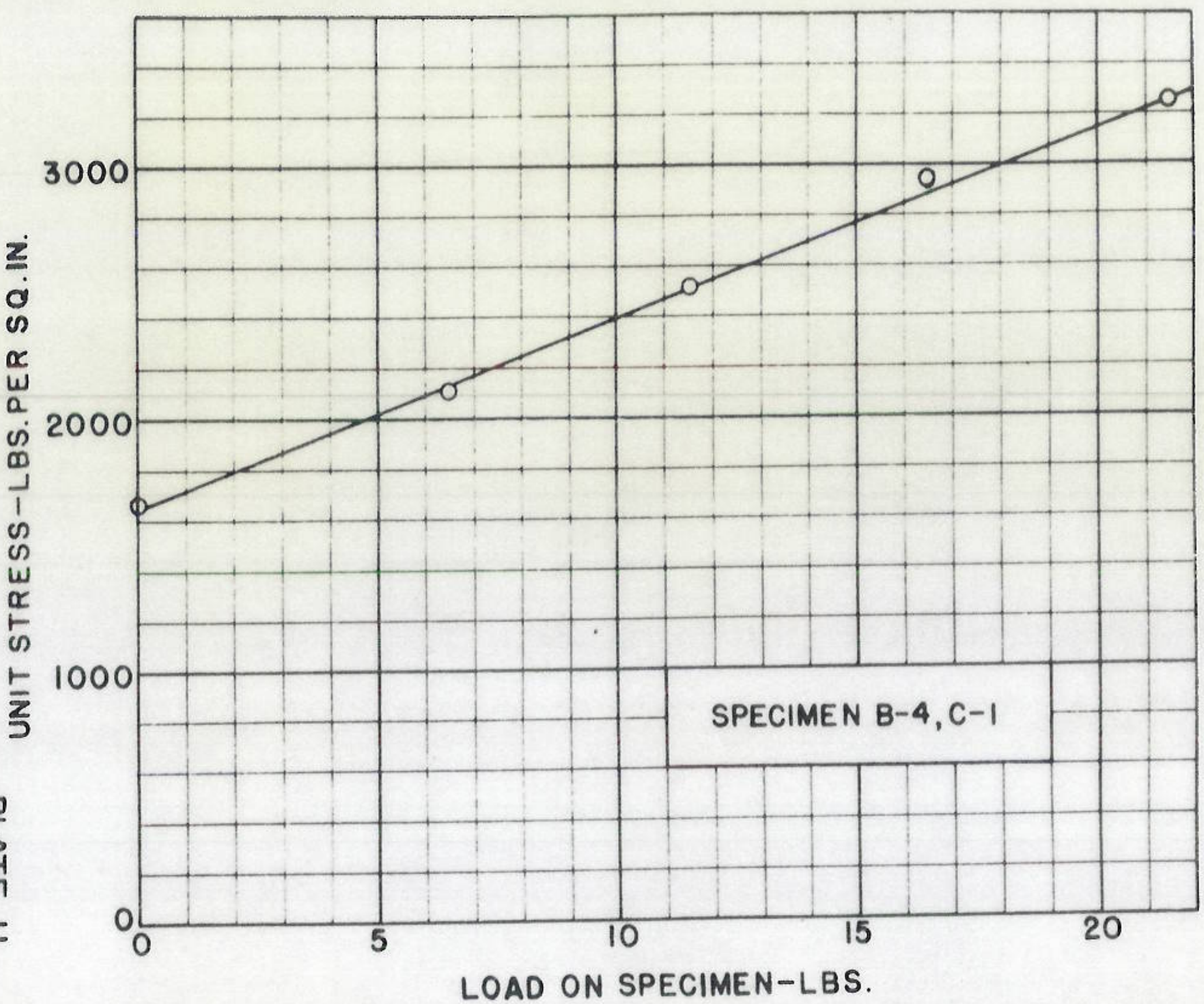
3000
2000
1000
0
UNIT STRESS-LBS. PER SQ. IN.
0
5
10
15
20
LOAD ON SPECIMEN-LBS.
SPECIMEN B-4, C-1

PLATE II

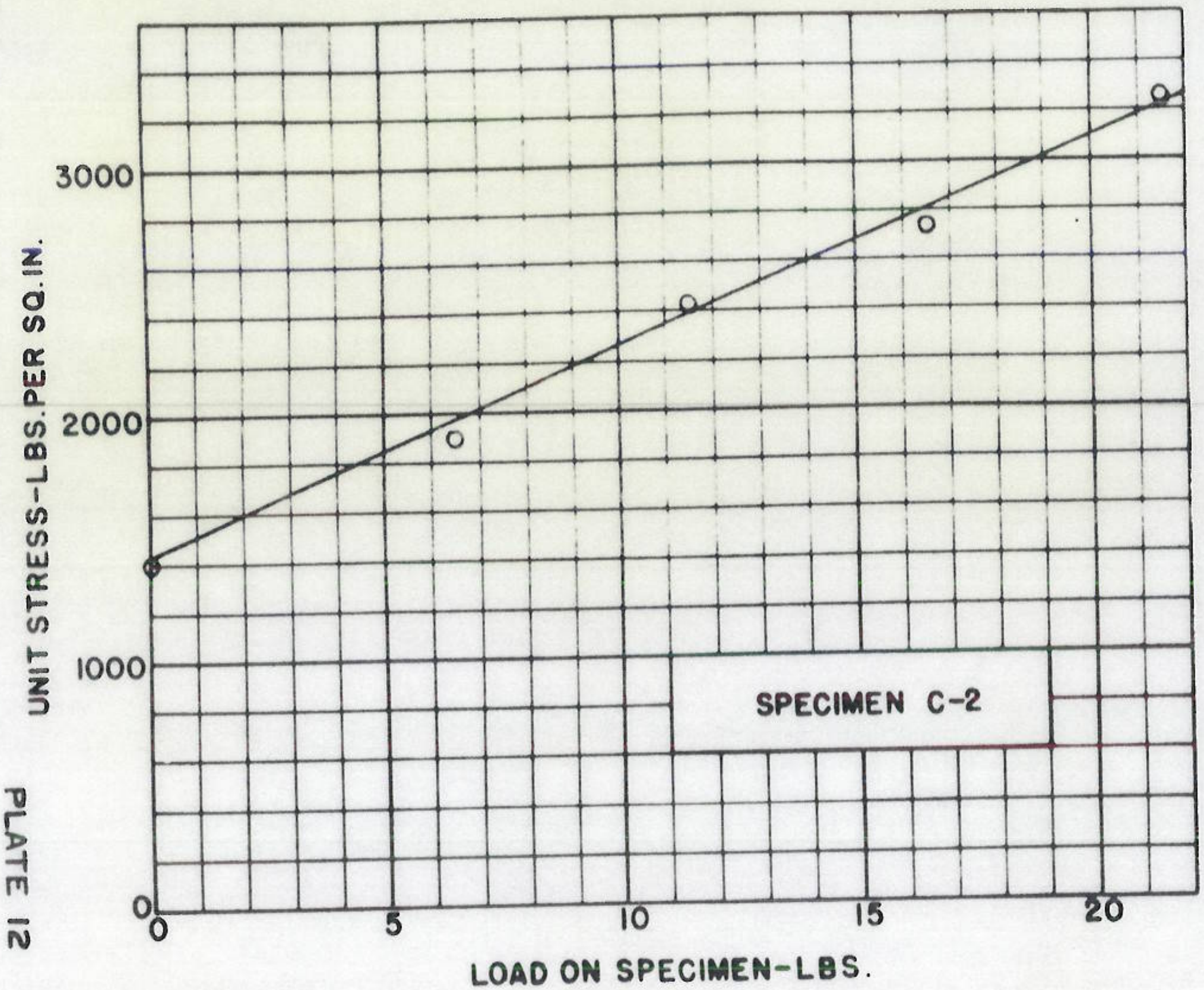
UNIT STRESS-LBS.PER SQ.IN.
3000
2000
1000
0
0
5
10
15
20
SPECIMEN C-2
LOAD ON SPECIMEN-LBS.

PLATE 12

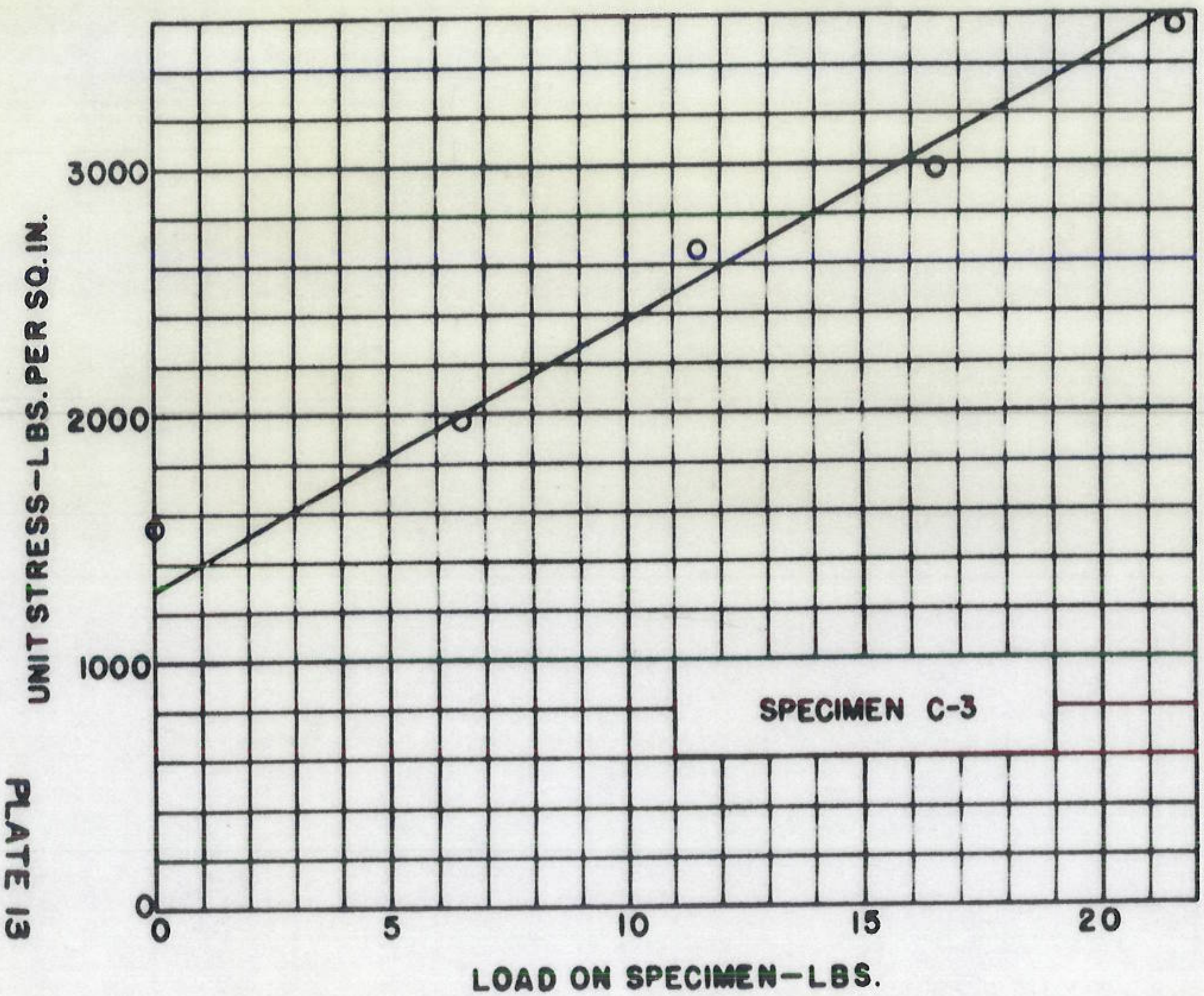
UNIT STRESS-LBS. PER SQ. IN.
3000
2000
1000
0
0
5
10
15
20
LOAD ON SPECIMEN—LBS.
SPECIMEN C-3

PLATE 13

Specimen No.	Radius - In. (1)	Amplitude - In. (2)	Load - Lbs. on Specimen (3)	Dynamometer Reading on Standard Specimen (Ave. of 4 Readings) (4)	Lbs.Load per unit Dynamometer Reading (5)	Load on Standard - Lbs. (4) x (5) (6)	Unit Stress in Specimen = (6) ÷ .0948 Area of Standard (7)	Thickness of Specimen Inches (8)	Thickness of Standard Inches (9)	Corrected Unit Stress in Specimen $\frac{(9)}{(8)}$ x (7) (10)
A-1	0.250	1.547	0	106.1	1.395	148.0	1564	.2520	.2535	1569
Inside of			6.5	138.3		192.9	2040			2050
Sharp Curve			11.5	160.6		224.0	2368			2380
			16.5	187.1		261.0	2760			2775
			21.5	212.3		296.0	3130			3146
A-1	0.688	1.547	0	-103.4		-144.2	-1521	.2520		-1530
Outside of			6.5	- 93.8		-130.8	-1380			-1388
Sharp Curve			11.5	- 89.0		-124.1	-1295			-1303
(-) = tension			16.5	- 79.9		-111.4	-1175			-1182
			21.5	{ -56.5		{ -78.8	{ -831			{ -835
				-67.7		-94.4	-997			-1102
				-76.4 }		- 106.5 }	-1124 }			-1131 }
A-1	1.500	1.547	0	122.5		170.8	1803	.2510		1822
Inside of	and		6.5	148.9		207.5	2190			2210
Large Curve	infinite		11.5	184.0		256.5	2708			2735
			16.5	199.4		278.0	2938			2968
			21.5	221.5		309.0	3260			3290
A-1	2.040	1.547	0	-95.3		-132.9	-1404	.2510		-1418
Outside of	and		6.5	-77.9		-108.7	-1148			-1160
Large Curve	infinite		11.5	-56.5		-78.8	-832			-841
(-) = tension			16.5	-42.4		-59.1	-624			-630
			21.5	-31.2		-43.5	-459			-464
A-2	0.360	1.422	0	92.0		128.2	1356	.2525		1360
Inside of			6.5	108.2		151.0	1594			1600
Sharp Curve			11.5	125.5		175.0	1848			1853
			16.5	138.5		193.2	2040			2048
			21.5	170.2		237.3	2505			2513
A-2	0.840	1.422	0	-88.3		-123.1	-1300	.2530		-1303
Outside of			6.5	-57.4		-80.0	-845			-847
Sharp Curve			11.5	-49.0		-68.3	-722			-724
(-) = tension			16.5	-45.1		-62.9	-665			-667
			21.5	-38.9		-54.2	-573			-574
A-2	1.440	1.422	0	95.2		132.8	1400	.2520		1409
Inside of	and		6.5	116.5		162.4	1716			1727
Large Curve	infinite		11.5	131.1		182.9	1930			1941
			16.5	147.1		205.0	2166			2178
			21.5	167.9		234.0	2472			2485
A-2	1.660	1.422	0	-42.9		-59.8	-631	.2520		-635
Outside of	and		6.5	-35.3		-49.2	-519			-522
Large Curve	infinite		11.5	-28.5		-39.7	-419			-421
(-) = tension			16.5	-25.4		-35.4	-374			-375
			21.5	-20.6		-28.7	-303			-305

PLATE 14

Specimen No.	Radius - In. (1)	Amplitude - In. (2)	Load - Lbs. on Specimen (3)	Dynamometer Reading on Standard Specimen (Ave. of 4 Readings) (4)	Lbs. Load per Unit Dynamometer Reading (5)	Load on Stand. - Lbs. 4 x 5 (6)	Unit Stress in Spec. = 6 .0948 Area of Stand. (7)	Thickness of Spec. In. (8)	Thickness of Stand. In. (9)	Corrected Unit Stress in Spec. 9/8 x 7 (10)
B-1	0.100	1.375	0	37.5	1.395	52.31	552	.2460	.2535	567
			6.5	101.5		141.59	1494			1539
			11.5	131.5		183.44	1935			1994
			16.5	166.3		231.99	2447			2522
			21.5	201.0		280.40	2958			3048
B-2	0.200	1.375	0	51.5		71.91	759	.2515		765
			6.5	101.5		141.59	1494			1505
			11.5	124.5		173.68	1832			1847
			16.5	159.3		222.22	2344			2363
			21.5	193.4		269.79	2846			2869
B-3	0.3125	1.375	0	115.2		160.70	1695	.2515		1709
			6.5	128.5		179.26	1891			1906
			11.5	180.0		251.00	2648			2669
			16.5	200.9		280.26	2956			2980
			21.5	232.0		323.64	3414			3441
B-4	0.500	1.375	0	112.0		156.24	1648	.2505		1668
			6.5	141.6		197.53	2084			2109
			11.5	168.7		235.34	2482			2512
			16.5	197.6		275.65	2908			2943
			21.5	217.9		303.97	3206			3244
B-5	0.750	1.375	0	81.1		113.13	1193	.2525		1196
			6.5	105.4		147.03	1551			1557
			11.5	122.0		170.19	1795			1802
			16.5	155.1		216.36	2282			2291
			21.5	186.1		259.61	2739			2750
B-6	1.000	1.375	0	79.1		110.34	1164	.2525		1169
			6.5	114.0		159.43	1682			1689
			11.5	136.0		189.72	2201			2009
			16.5	164.0		228.78	2413			2423
			21.5	183.5		255.98	2700			2711
B-7	1.145	1.375	0	101.0		140.90	1486	.2500		1507
			6.5	115.0		160.43	1692			1716
			11.5	145.0		202.28	2134			2164
			16.5	167.0		232.97	2457			2491
			21.5	193.4		269.79	2846			2886
C-1	0.500	1.375	0	112.0		156.24	1648	.2505		1668
			6.5	141.6		197.53	2084			2109
			11.5	168.7		235.34	2482			2512
			16.5	197.6		275.65	2908			2943
			21.5	217.9		303.97	3206			3244
C-2	0.500	1.500	0	94.0		131.13	1383	.2515		1394
			6.5	127.9		178.42	1882			1897
			11.5	163.5		228.08	2406			2425
			16.5	184.6		257.52	2716			2738
			21.5	218.6		304.95	3217			3243
C-3	0.500	2.000	0	104.0		145.08	1530	.2520		1539
			6.5	133.3		185.95	1961			1973
			11.5	179.5		250.40	2641			2657
			16.5	200.7		279.98	2953			2971
			21.5	240.0		334.80	3532			3553

PLATE 15

DIMENSIONS ON PLATES 16-20 ARE
FOR BRASS MASTER, i.e. 2 TIMES
CELLULOID MODEL OR 4 TIMES STEEL.

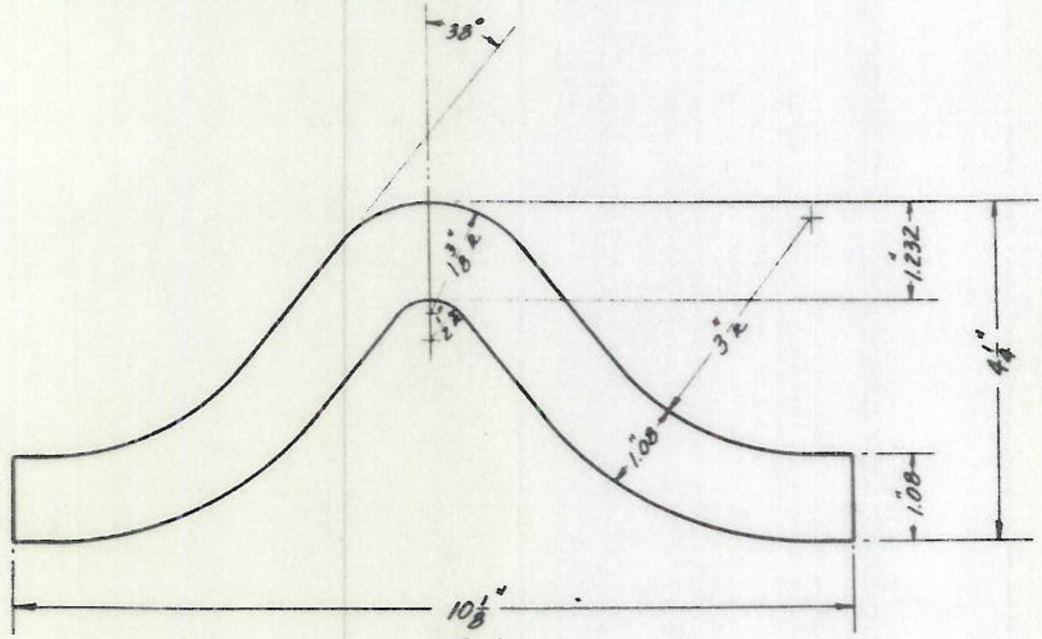

A-1

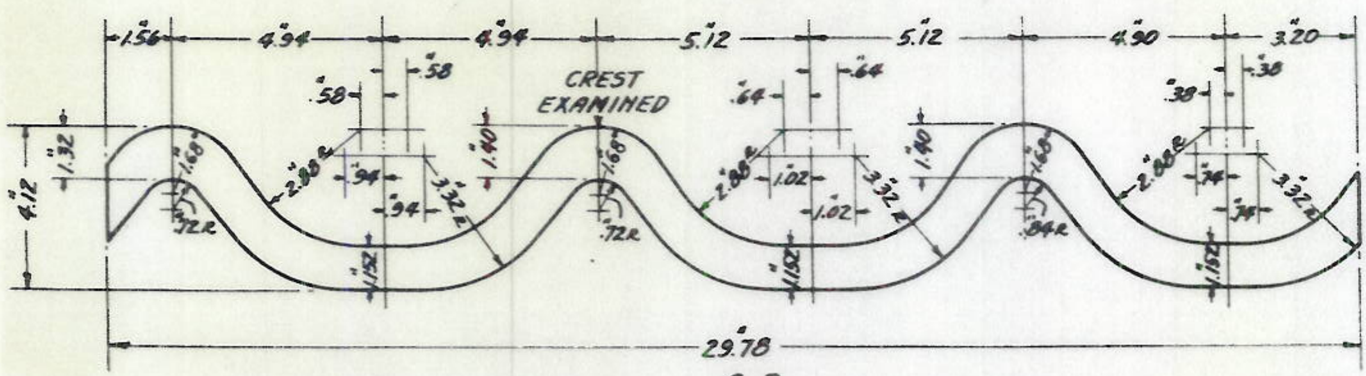

A-2

PLATE 16

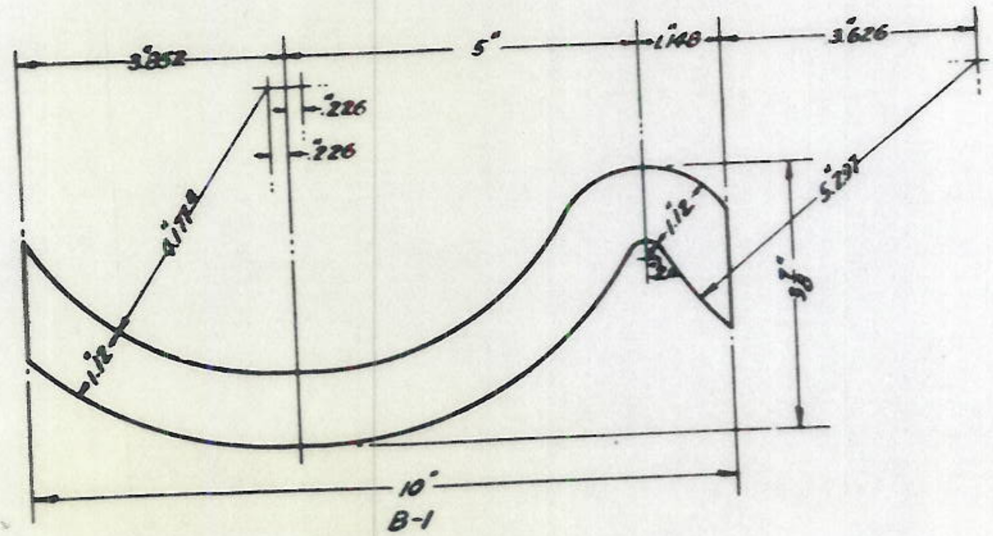

B-1

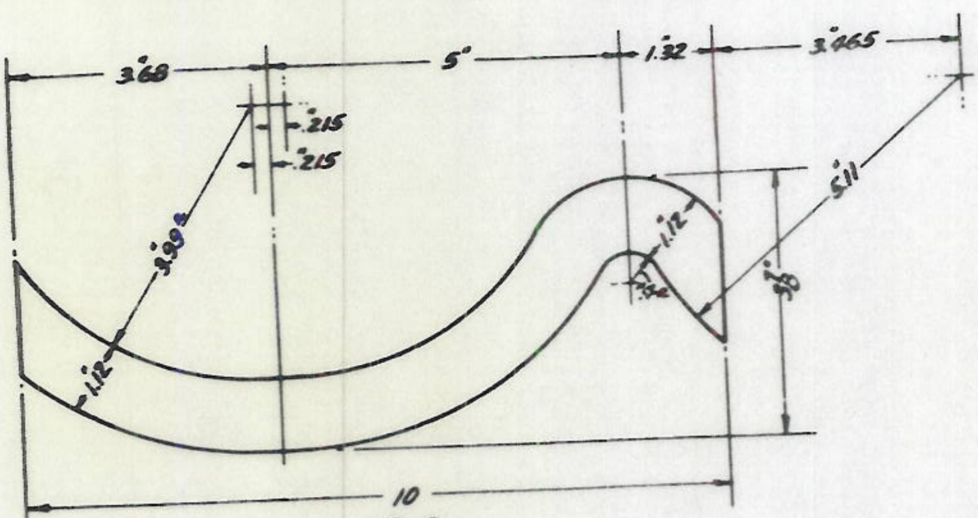

B-2

PLATE 17

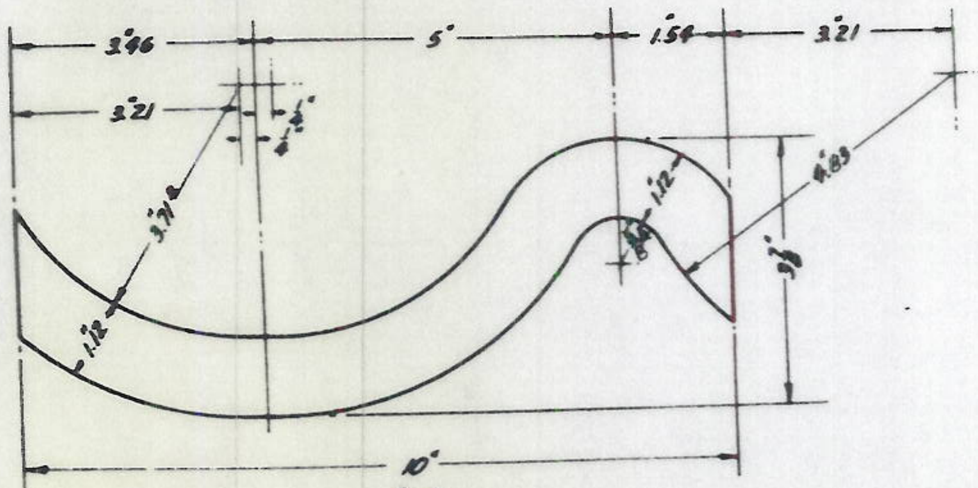

B-3

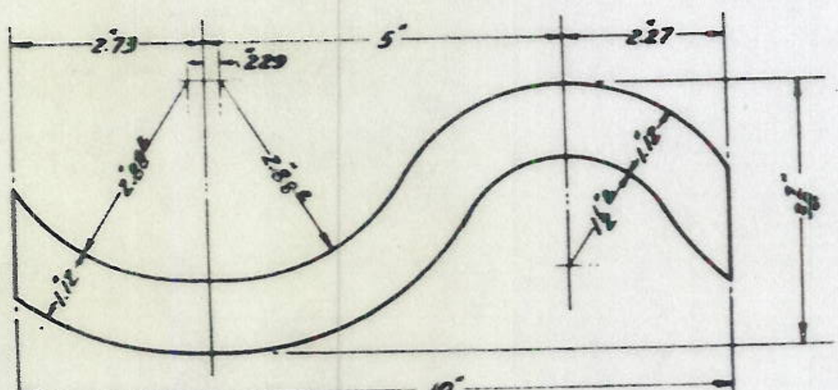

B-5

PLATE 18

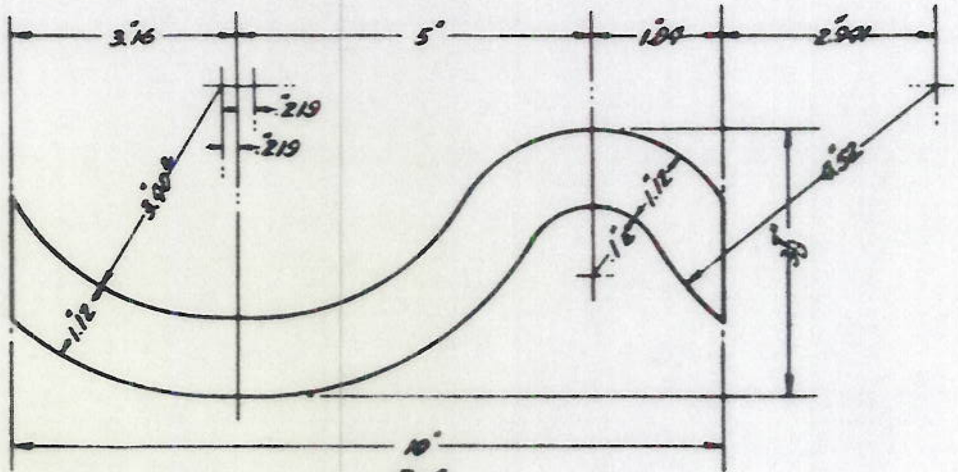

B-4
C-1

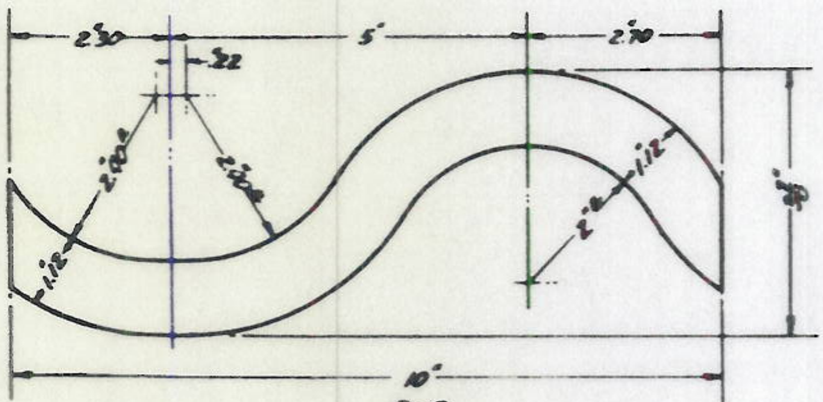

B-6

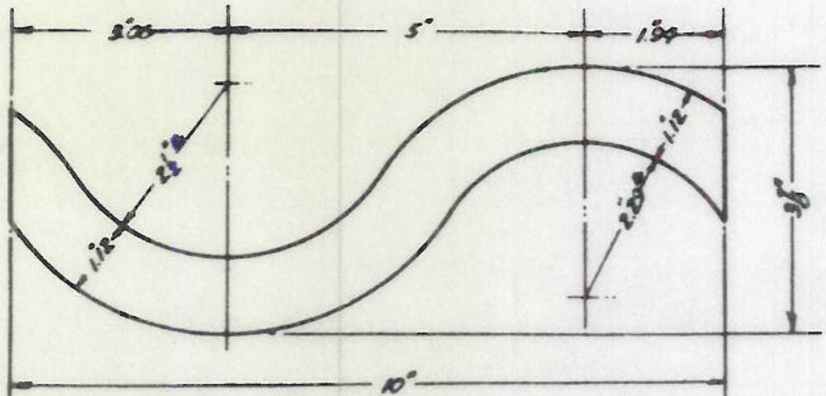

B-7

PLATE 19

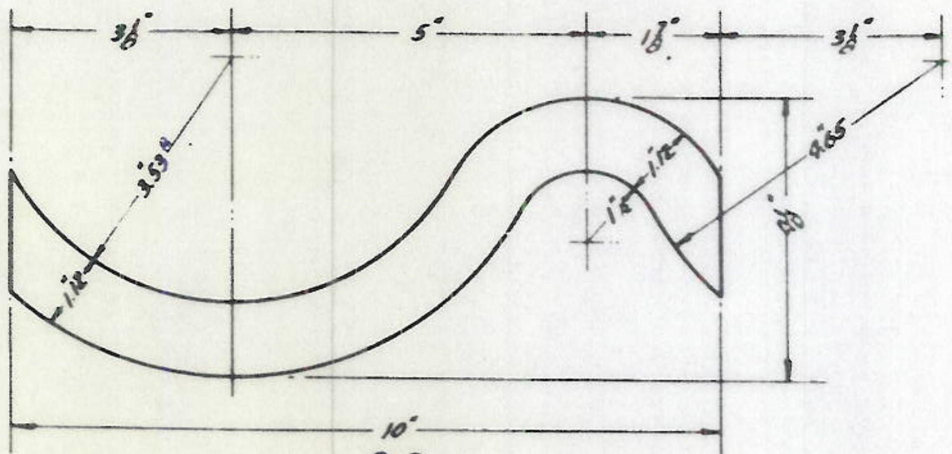

C-2

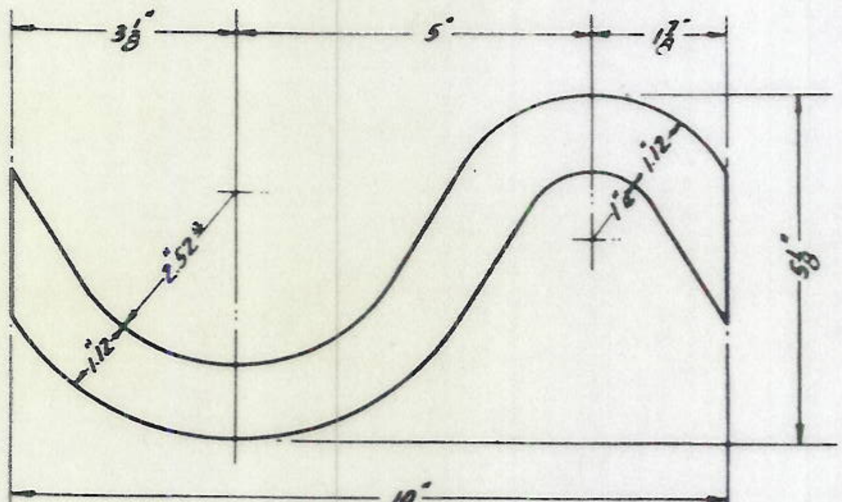

C-3

PLATE 20

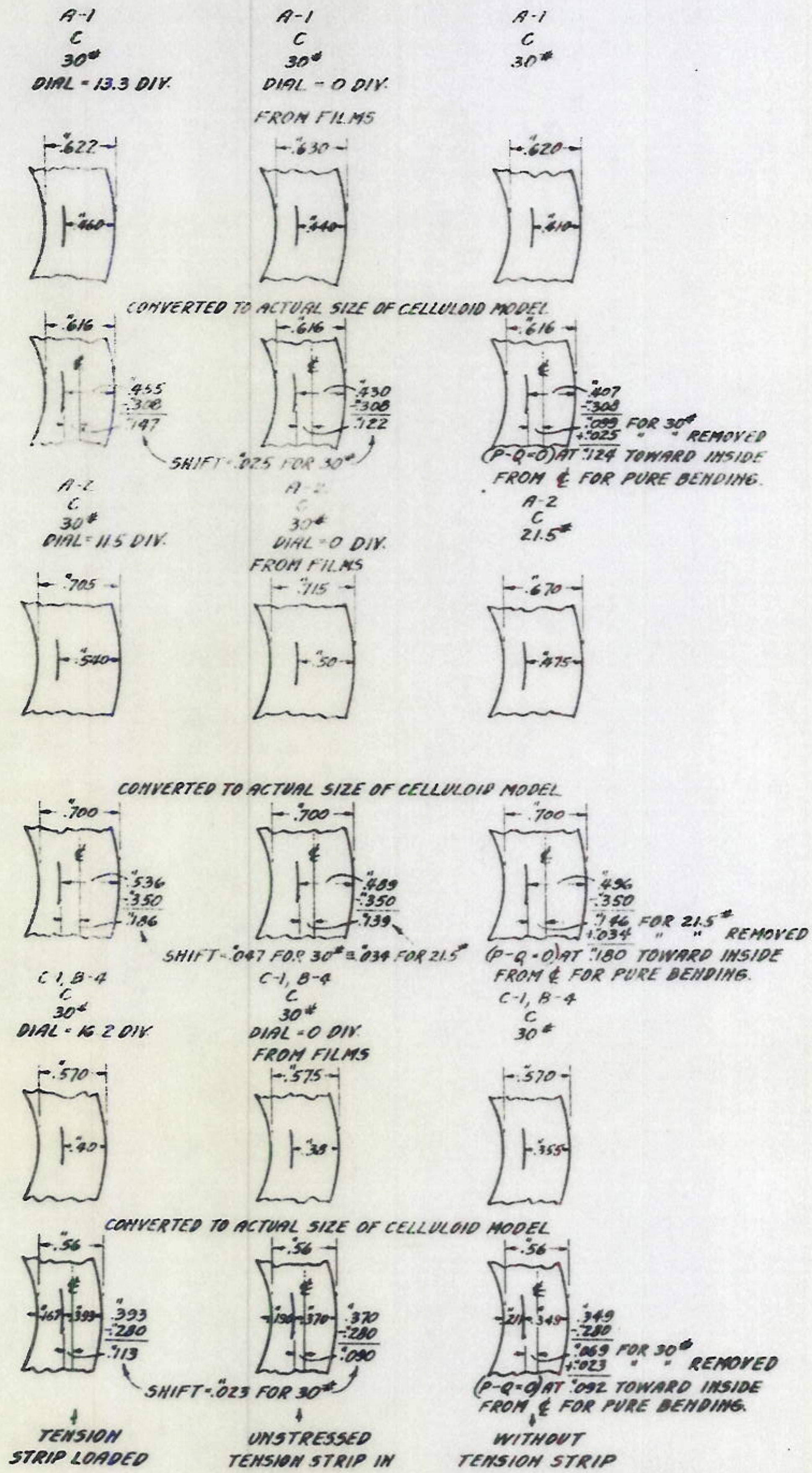

A-1
C
30#
DIAL = 13.3 DIV.
A-1
C
30#
DIAL - O DIV.
A-1
C
30#
FROM FILMS
CONVERTED TO ACTUAL SIZE OF CELLULOID MODEL
SHIFT = .025 FOR 30#
(P-Q=O) AT .124 TOWARD INSIDE FROM ℄ FOR PURE BENDING.
A-2
C
30#
DIAL = 11.5 DIV.
A-2
C
30#
DIAL = O DIV.
A-2
C
21.5#
FROM FILMS
CONVERTED TO ACTUAL SIZE OF CELLULOID MODEL
SHIFT = .047 FOR 30# = .034 FOR 21.5#
(P-Q=O) AT .180 TOWARD INSIDE FROM ℄ FOR PURE BENDING.
C-1, B-4
C
30#
DIAL = 16.2 DIV.
C-1, B-4
C
30#
DIAL = O DIV.
C-1, B-4
C
30#
FROM FILMS
CONVERTED TO ACTUAL SIZE OF CELLULOID MODEL
SHIFT = .023 FOR 30#
(P-Q=O) AT .092 TOWARD INSIDE FROM ℄ FOR PURE BENDING.
TENSION STRIP LOADED
UNSTRESSED TENSION STRIP IN
WITHOUT TENSION STRIP
1 DIAL DIVISION = 1.395#

PLATE 20A

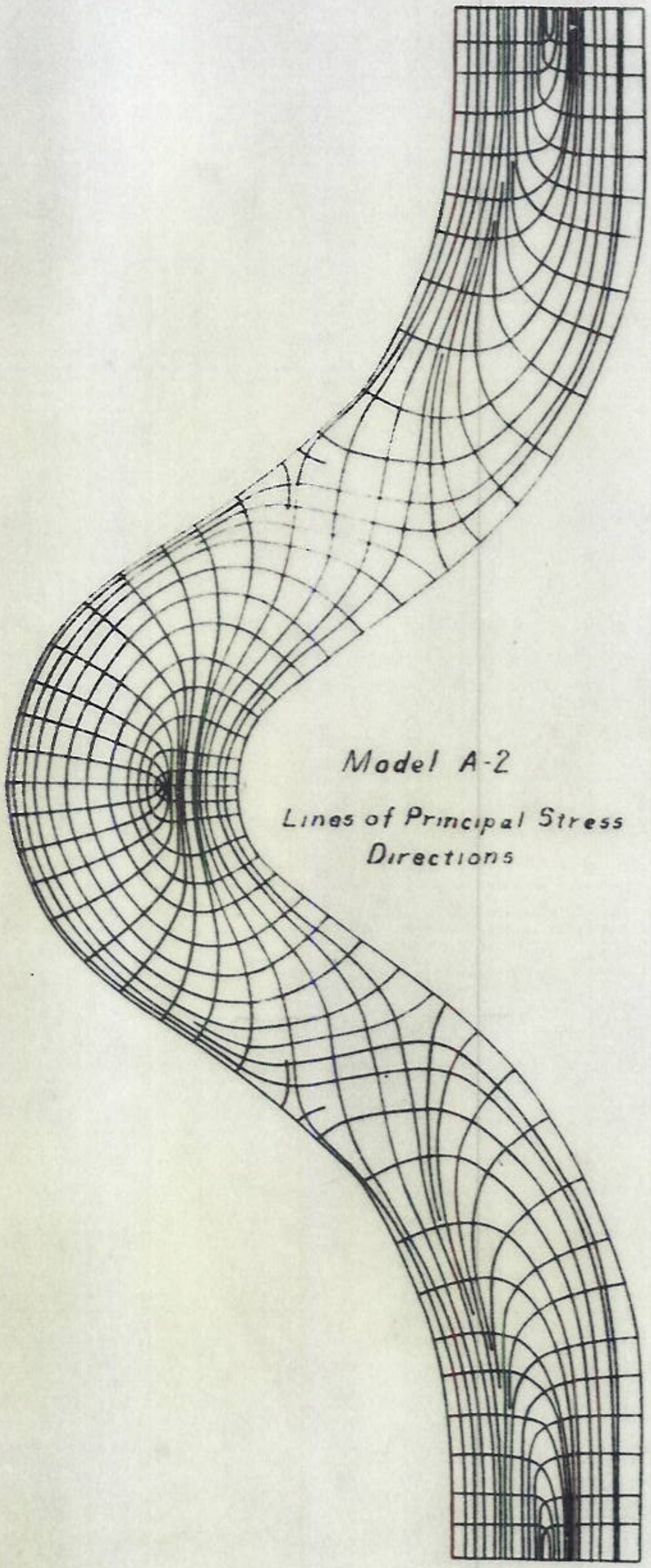
Model A-2
Lines of Principal Stress
Directions

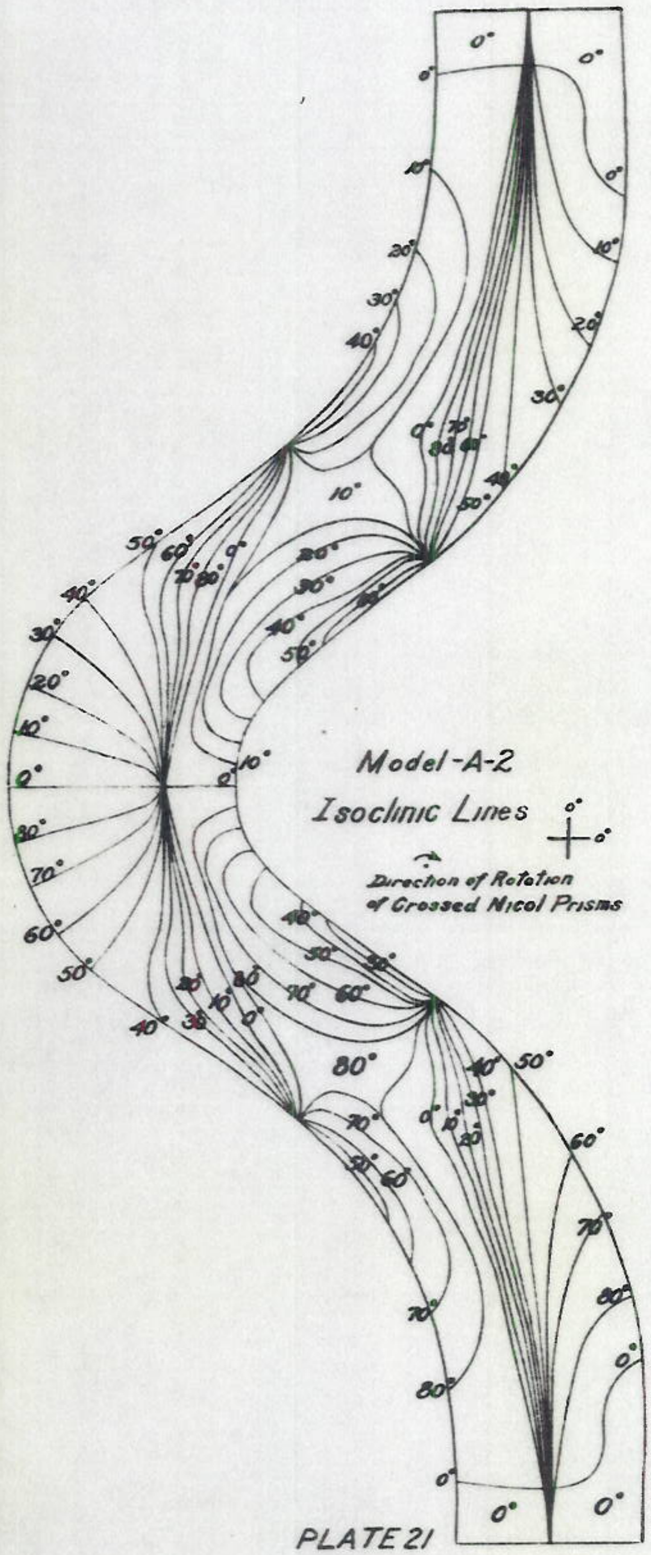
Model-A-2
Isoclinic Lines
Direction of Rotation
of Crossed Nicol Prisms

PLATE 21

Model A2

Scale: 10" = 1"
" 1" = 100#/□

From Planimeter

Area under tension side of P curve = 10.35 sq. in. = P_1
" " compression " " " " = -7.45 " " = P_2
Direct tension = 2.90 " "

1 sq. in = 100#/□ × 0.10" × 0.253" = 2.53 pounds
(thickness of model)

∴ 2.90 × 2.53 #/□ = 7.337 pounds direct stress
or 41.42 #/□ average

Load Increment = 20.8 pounds
or 112.93 #/□ average

Assume: { Curve of "P-Q" values across section au. Linear change of r from each edge to P-Q=0, i.e. point k.

P_1 = 10.35 □ × 2.53 = 26.19#
P_2 = 7.45 □ × 2.53 #/□ = 18.85#
$P_1 - P_2$ = 26.19 − 18.85 = 7.34#

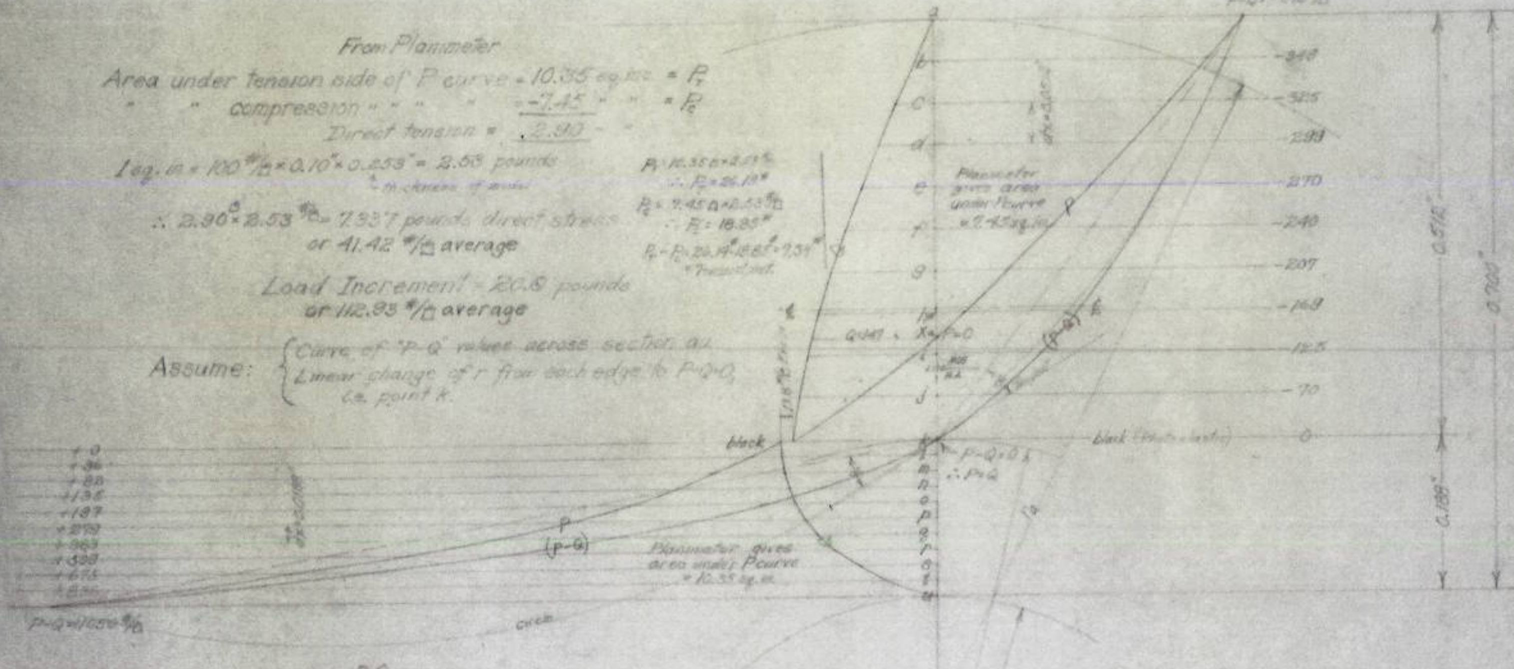

$$dQ = -\frac{P-Q}{r}\,dx$$

Point	P-Q	Mean P-Q #/□	Radius r"	Mean r"	dx"	dQ #	Q #/□	P #/□
a	-370	—	0.844	—	—	—	0.0	-370.0
b	-348	-359.5	0.807	0.826	+0.0512	+22.3	+22.3	-325.7
c	-325	-337	0.771	0.789	+0.0512	+21.9	+44.2	-280.8
d	-299	-312	0.734	0.752	+0.0512	+21.2	+65.4	-233.6
e	-270	-284.5	0.698	0.716	+0.0512	+20.3	+85.7	-184.3
f	-240	-255	0.661	0.680	+0.0512	+19.2	+104.9	-135.1
g	-207	-223.5	0.624	0.642	+0.0512	+17.8	+122.7	-84.3
h	-169	-188	0.588	0.606	+0.0512	+15.9	+138.6	-30.4
i	-125	-147	0.551	0.570	+0.0512	+13.2	+151.8	+26.8
j	-70	-97.5	0.515	0.533	+0.0512	+9.4	+161.2	+91.2
k	0	-70	0.478	0.496	+0.0512	+7.2	+168.4	+168.4
k	+0	+36	0.478	0.472	-0.0188	+1.4	+182.2	+182.2
l	+36	+59	0.465	0.458	-0.0188	+2.4	+180.8	+216.8
m	+82	+108.5	0.451	0.444	-0.0188	+4.6	+178.4	+260.4
n	+135	+166	0.438	0.431	-0.0188	+7.2	+173.8	+308.8
o	+197	+238	0.424	0.418	-0.0188	+10.7	+166.6	+363.6
p	+279	+331	0.411	0.404	-0.0188	+15.4	+155.9	+434.9
q	+383	+446	0.398	0.391	-0.0188	+21.4	+140.5	+523.5
r	+509	+592	0.384	0.378	-0.0188	+29.4	+113.1	+622.1
s	+675	+755.5	0.371	0.364	-0.0188	+39.0	+89.7	+764.7
t	+836	+943	0.357	0.350	-0.0188	+50.7	+50.7	+886.7
u	+1050	—	0.344	—	—	—	0.0	+1050.0

P = 0 @ X =

$$\frac{30.4}{30.4+26.8} \times 0.0512 + 7 \times 0.0512" = 0.3856" \text{ in from a}$$

Center for r_a = 0.844"
Center for r_k = 0.478"
Center for r_u = 0.344"

Radius of Neutral Axis

r_a = 0.844"
r_u = 0.344"
0.500" = change in r

$r_k = r_{N.A.} = r_u + \frac{.188"}{.700"} \times .500" =$
0.134" + 0.344" = 0.478"

0.500"
−0.134" = change in r from k to u
0.366" = change in r from a to k

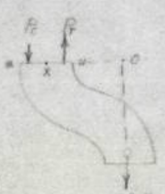

For Static Equilibrium

$\Sigma M_o = 0$ i.e. $P_c \times arm_c + P_T \times arm_T = 0$

$\Sigma F_Y = 0$ Does not check

P_c from Σ rectangles + Σ triangles gives
−16.5183# − 2.8364 = −19.3547# ∴ Checks

PLATE 22

PLATE 22

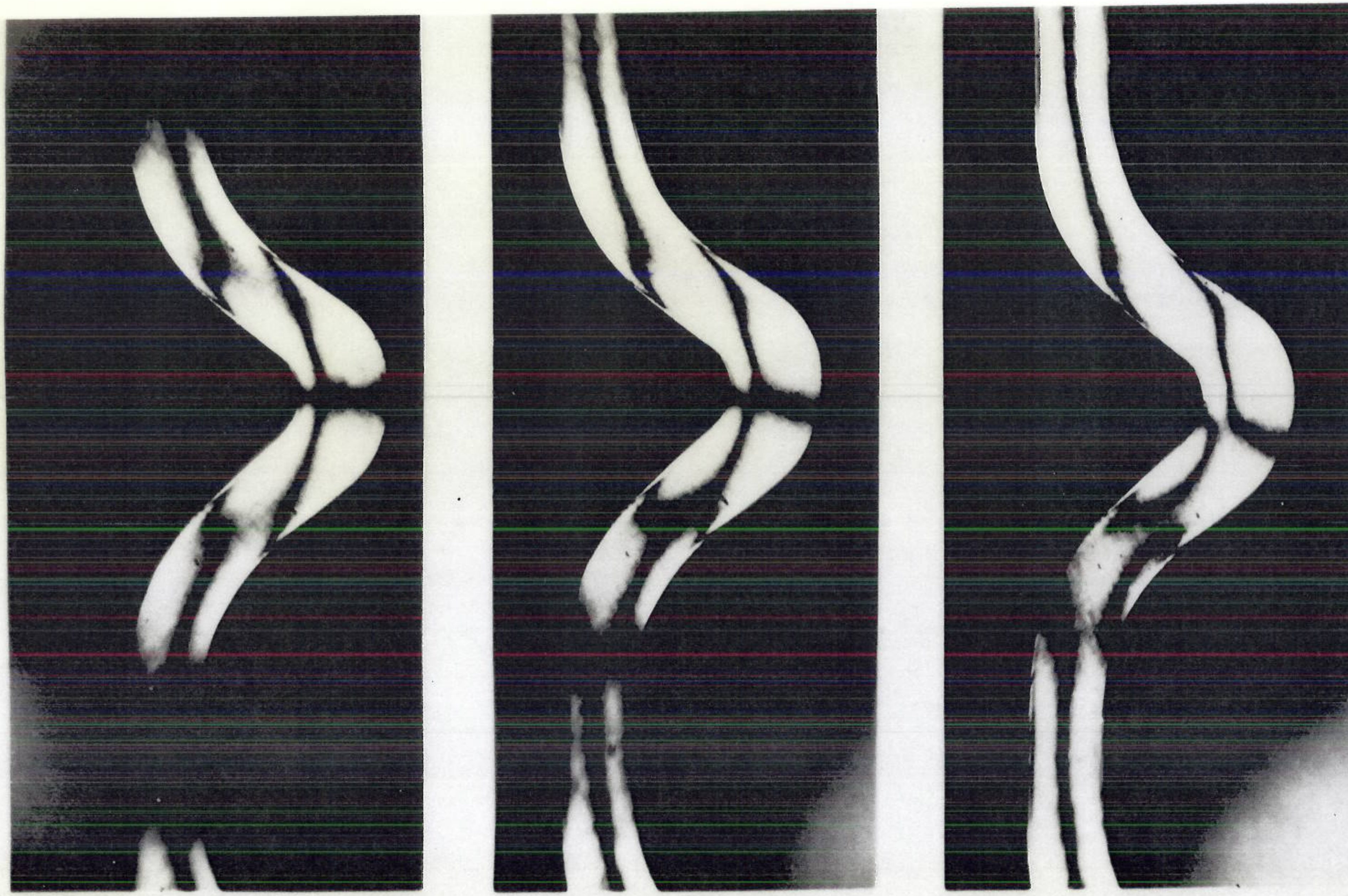

A-2; 0° A-2; 10° A-2; 20°

Plane Polarized Light Showing Isoclinic Lines

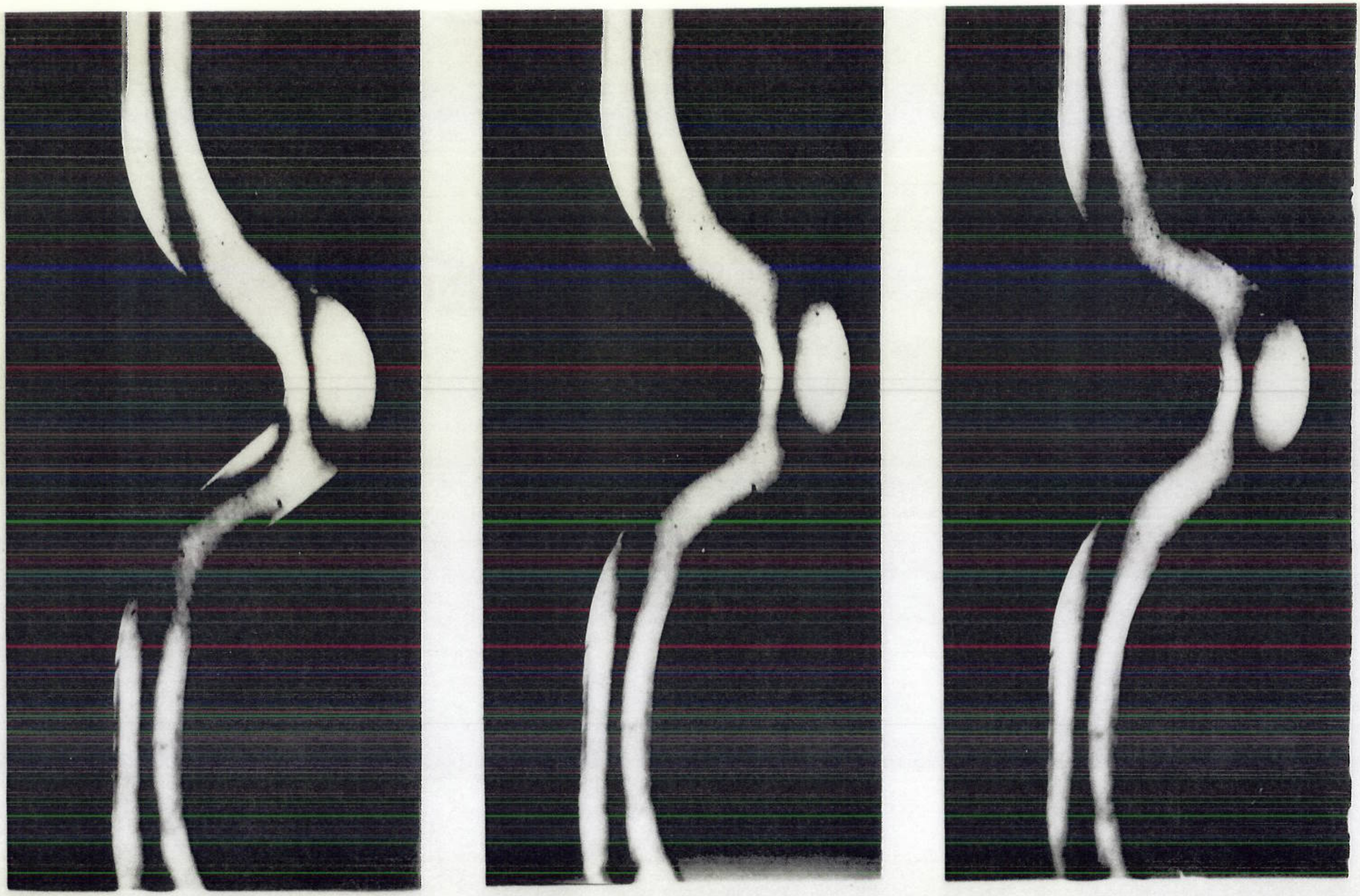

A-2; 30　　A-2; 40°　　A-2; 50°

Plane Polarized Light Showing Isoclinic Lines

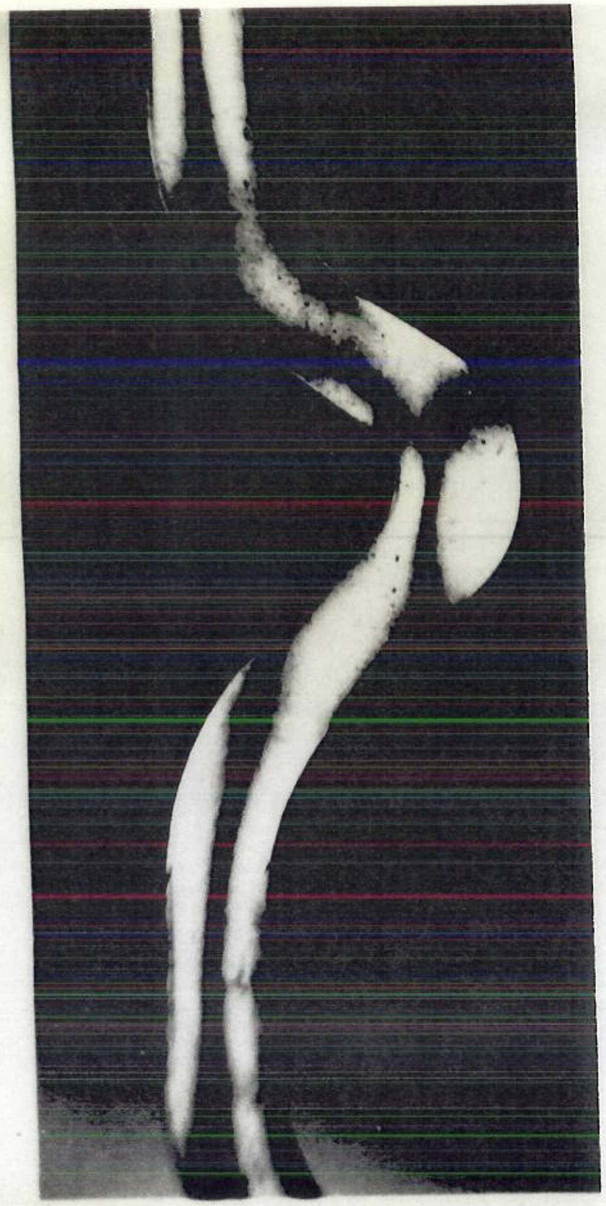

A-2; 60°

A-2; 70°

A-2; 80°

Plane Polarized Light Showing Isoclinic Lines

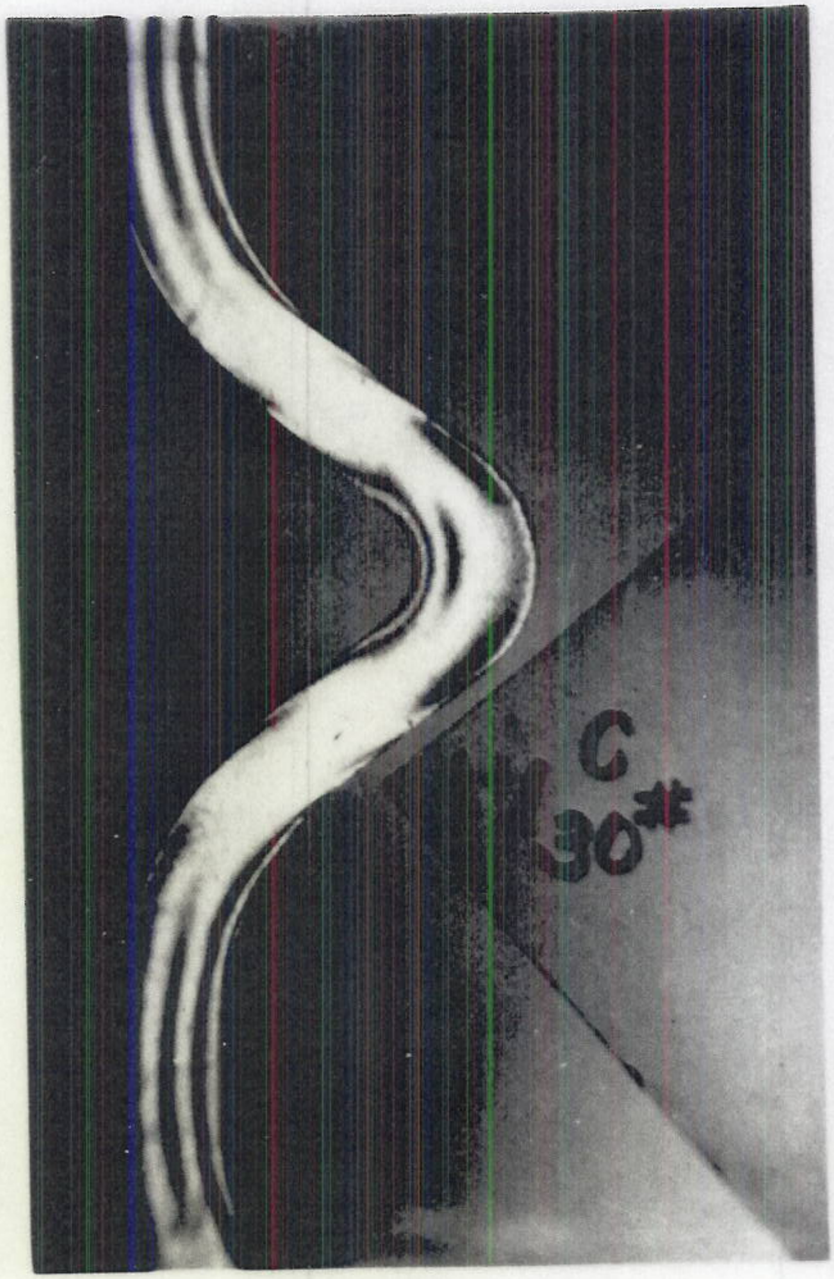

Specimen A-1
Circularly Polarized
Light

Specimen A-1

with unloaded compensator strip

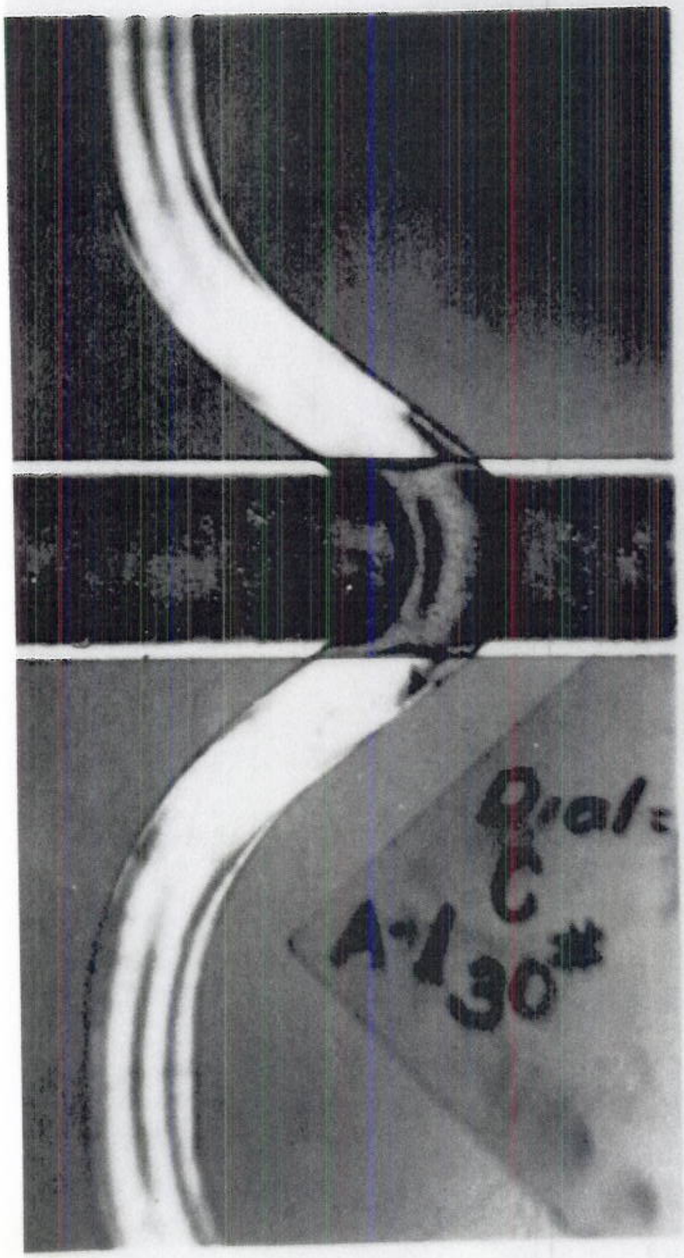

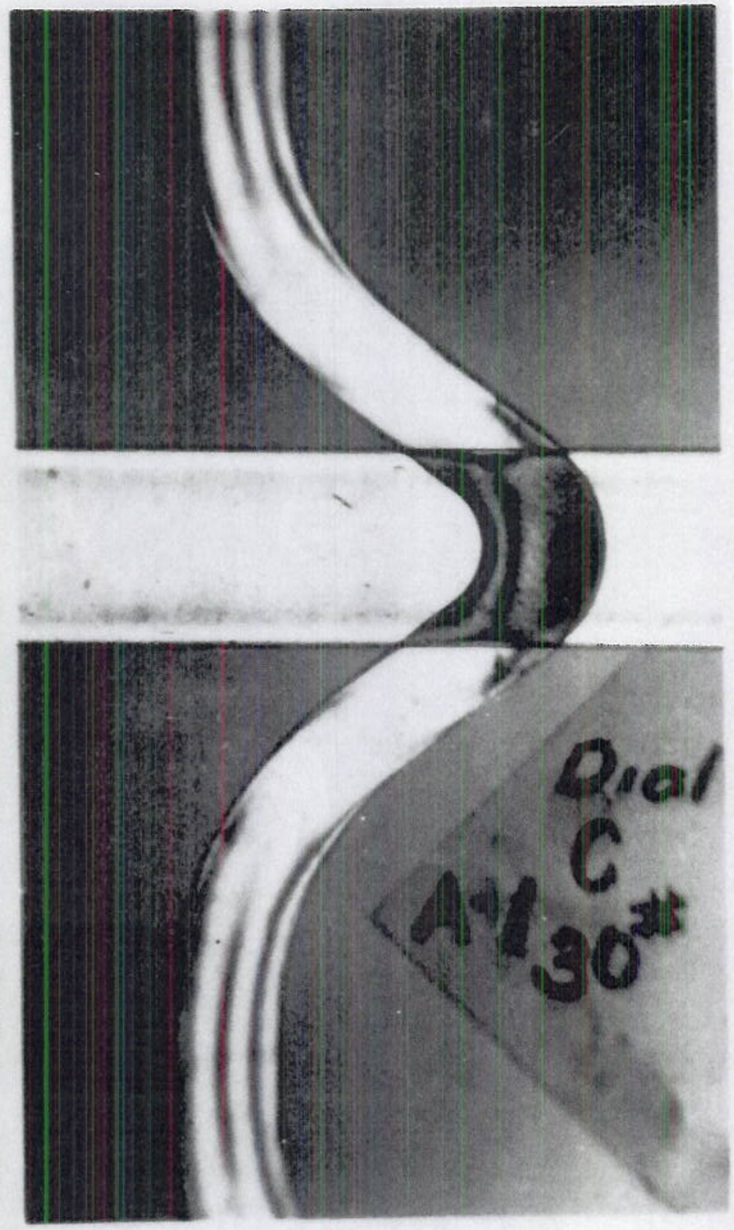

Specimen A-1

with tension strip loaded to compensate for direct stress uniformly distributed over section of symmetry

Specimen A-2
with unloaded compensator strip

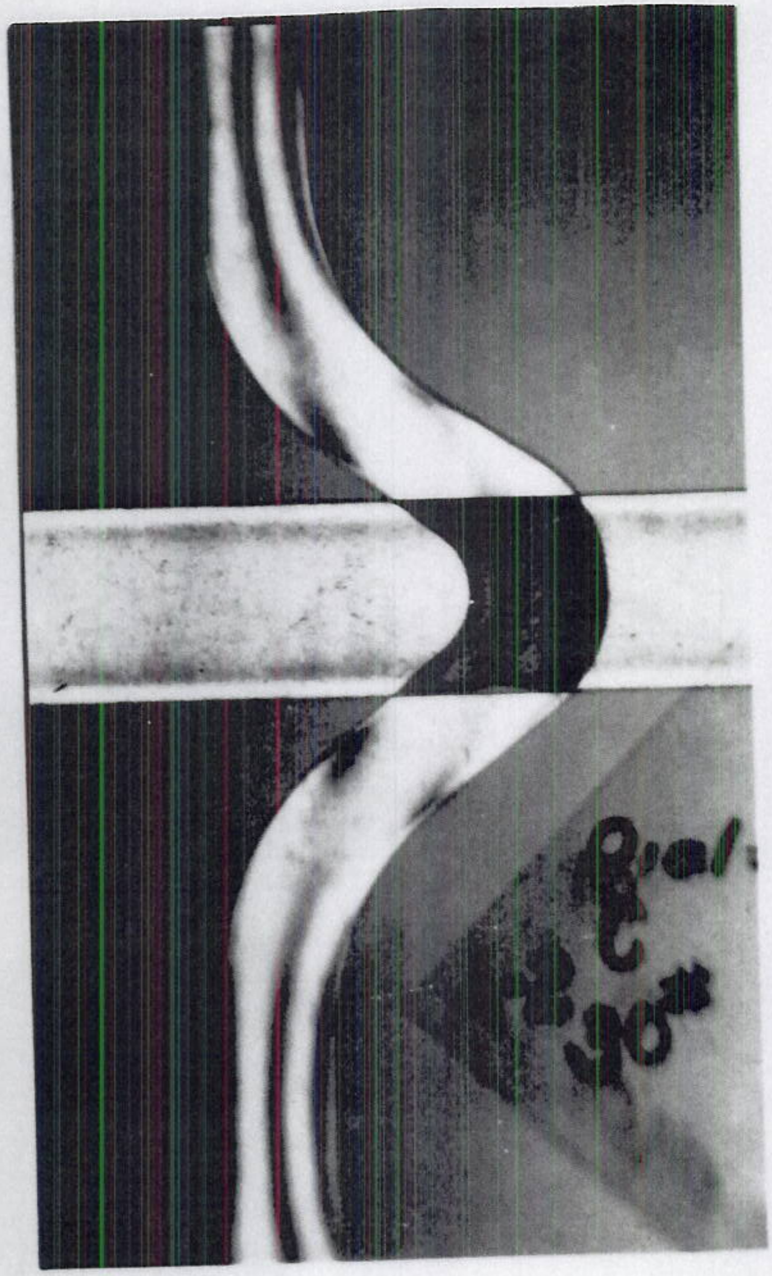

Specimen A-2
with tension strip loaded to compensate for direct stress uniformly distributed over section of symmetry

Plate 29

Specimen C-1;B-4
with unloaded compensator strip

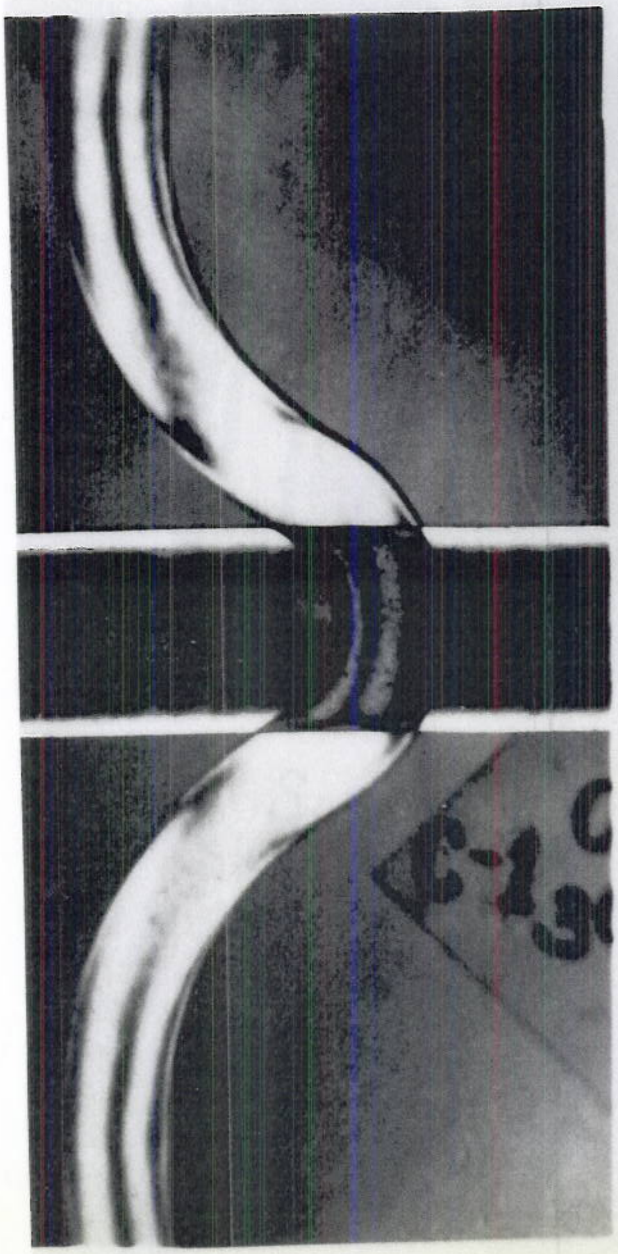

Specimen C-1;B-4
with tension strip loaded to compensate for direct stress uniformly distributed over section of symmetry

Specimen B-3
Circularly Polarized
Light

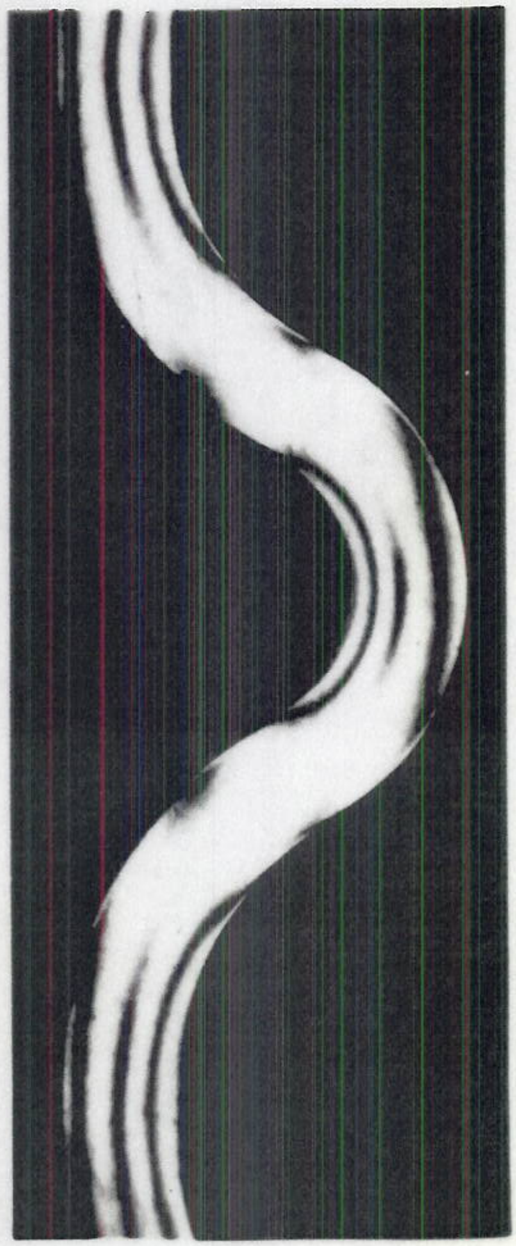

Specimen B-5
Circularly Polarized
Light

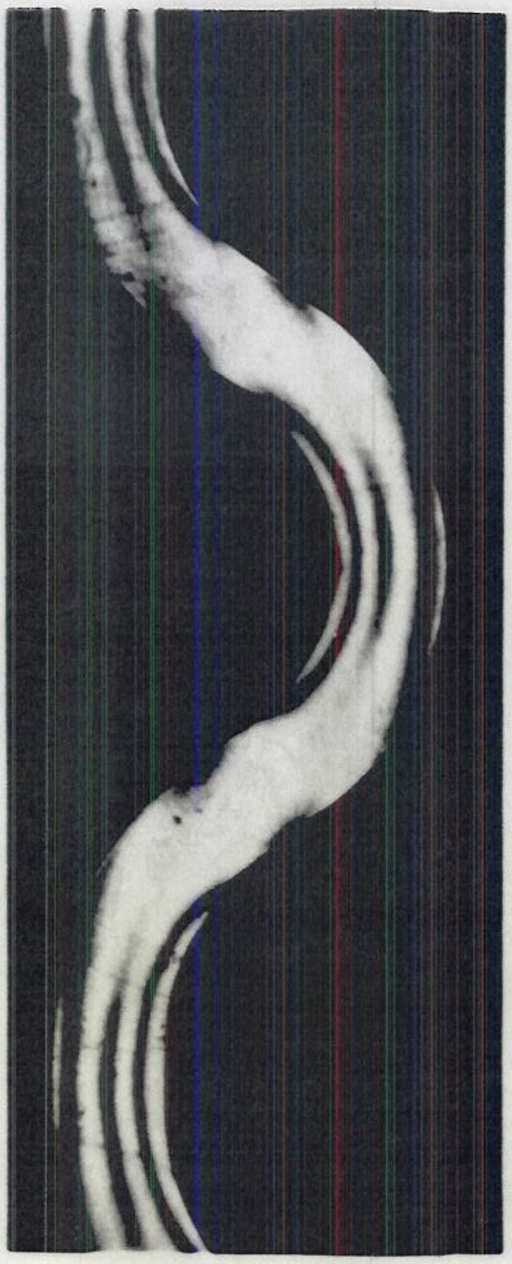

Specimen B-6
Circularly Polarized
Light

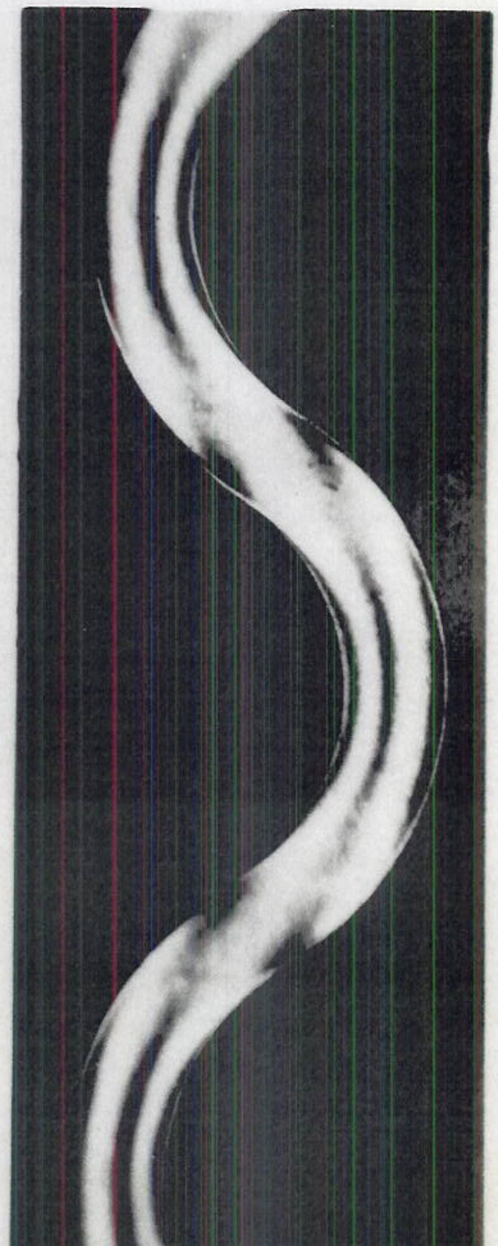

Specimen B-7
Circularly Polarized
Light

C-1; B-4

C-2

C-3

Plate
35

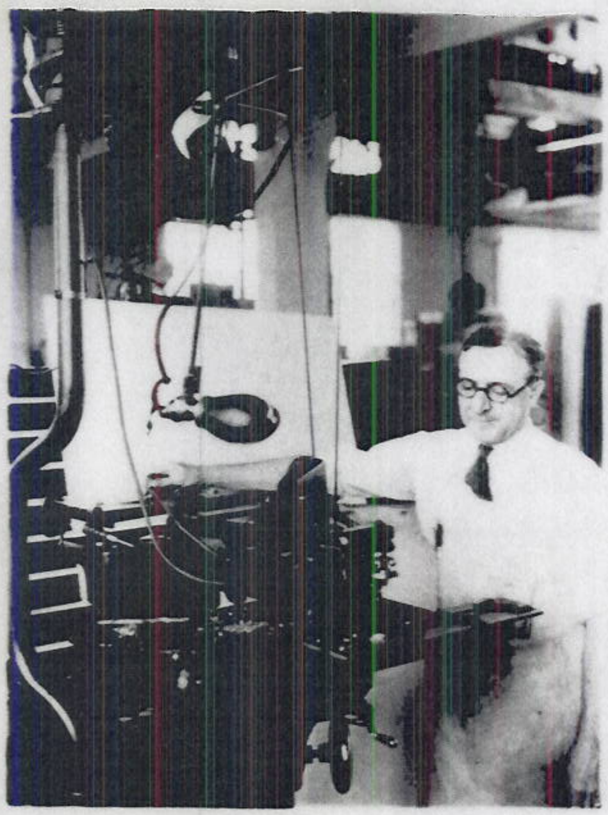

Note

Brass Master at "A"

Cutting Specimen on Engraving Machine

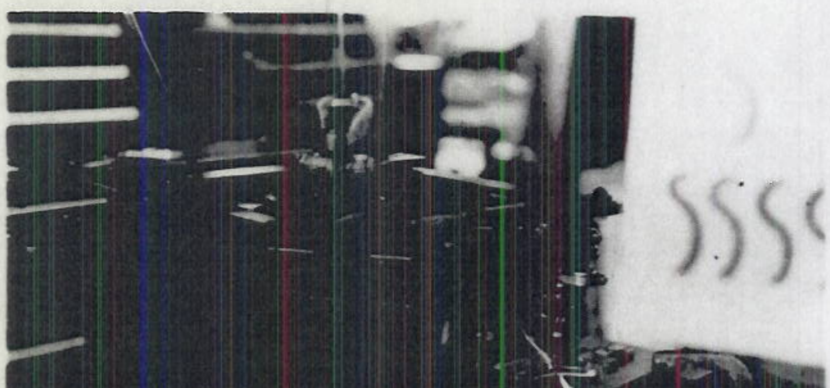

Note $\frac{1}{8}$" diam. Side Milling Tool at "B" and Wave Length Rods at "C"

Plate 37